Copper(II) Complexes with Highly Water-Soluble L- and D-Proline Thiosemicarbazone Conjugates as Potential Inhibitors of Topoisomerase IIα

Felix Bacher,[a] Éva A. Enyedy[b] Nóra V. Nagy,[c] Antal Rockenbauer,[c] Gabriella M. Bognár,[b] Robert Trondl,[a] Maria S. Novak,[a] Erik Klapproth,[a] Tamás Kiss,[b,d] Vladimir B. Arion*[a]*

[a]*University of Vienna, Institute of Inorganic Chemistry, Währinger Strasse 42, A-1090 Vienna, Austria,* [b]*Department of Inorganic and Analytical Chemistry, University of Szeged, Dóm tér 7. H-6720 Szeged, Hungary,* [c]*Institute of Molecular Pharmacology, Research Centre for Natural Sciences, Hungarian Academy of Sciences, Pusztaszeri út 59-67, H-1025, Budapest, Hungary,* [d]*HAS-USZ Bioinorganic Chemistry Research Group, Dóm tér 7. H-6720 Szeged, Hungary*

Keywords: Thiosemicarbazones, Solution equilibrium, Stability constants, Antitumor activity, Topoisomerase IIα

Abstract

Two proline-thiosemicarbazone bioconjugates with excellent aqueous solubility, namely 3-methyl-(*S*)-pyrrolidine-2-carboxylate-2-formylpyridine thiosemicarbazone (L-Pro-FTSC or (*S*)-H_2L) and 3-methyl-(*R*)-pyrrolidine-2-carboxylate-2-formylpyridine thiosemicarbazone (D-Pro-FTSC or (*R*)-H_2L) have been synthesized and characterized by elemental analysis, one- and two-dimensional ^1H and ^{13}C NMR spectroscopy and ESI mass spectrometry. The complexation behavior of L-Pro-FTSC with copper(II) in aqueous solution and in 30% (w/w) dimethyl sulfoxide/water mixture has been studied via pH-potentiometry, UV−vis spectrophotometry, EPR, ^1H NMR spectroscopy and spectrofluorometry. By the reaction of copper(II) acetate with (*S*)-H_2L and (*R*)-H_2L in water the complexes [Cu(*S*,*R*)-L] and [Cu(*R*,*S*)-L] have been synthesized and comprehensively characterized. An X-ray diffraction study of [Cu(*S*,*R*)-L] showed the formation of a square-pyramidal complex with the bioconjugate acting as a pentadentate ligand. Both copper(II) complexes displayed antiproliferative activity in CH1 ovarian carcinoma cells and inhibited the Topoisomerase IIα activity in a DNA plasmid relaxation assay.

Introduction

Thiosemicarbazones (TSCs) are efficient metal chelators and their coordination chemistry is well developed,[1,2] especially for the first row transition metal ions, e.g. iron(II), copper(II) and zinc(II).[3] High affinity to certain metal ions also makes them useful for analytical purposes.[4]A salient feature of TSCs is their broad-spectrum biological activity, e.g., antineoplastic, antimalarial, antibacterial, antiviral and antifungal.[2,5] Their anticancer activity was discovered in the 1950s when some compounds of this class were found to possess antileukemic properties in a mice model.[6] To date the most studied representative is 3-aminopyridine-2-carboxaldehyde TSC (3-AP or Triapine), which has already been evaluated in several clinical phase I and phase II trials. Unfortunately, Triapine exhibited severe side effects like methemoglobinemia, acute hypoxia and neutropenia, while only little response was observed.[7–11] Ribonucleotide reductase (RNR), an enzyme catalyzing the rate determining step in DNA synthesis, namely the reduction of ribonucleotides to the corresponding deoxyribonucleotides by a radical mechanism, is most probably the main target for Triapine and related TSCs.[12–15] Although thiosemicarbazones are good iron chelators, iron removal seems not to be the only mechanism for the RNR inhibition, since desferrioxamine (DFO), a strong chelator applied for the treatment of iron

overload disease,[16] is a weaker RNR inhibitor and far less cytotoxic than Triapine and related TSCs.[17,18] In addition, it was also shown that the iron(II)-bis(Triapine) complex is a more active RNR inhibitor than the corresponding iron(III) complex, which is able to quench the tyrosyl radical in the active center of RNR due to the formation of reactive oxygen species (ROS).[19,20] Recently, it was reported that the tyrosyl radical may be quenched directly by the Fe(II) complex without the involvement of oxygen.[21] Another established target for some TSCs is Topoisomerase IIα (Topo IIα), an enzyme regulating DNA topology during cell division.[22–25] A series of α-*N*-heterocyclic TSCs exhibited strong affinity to the enzyme ATP binding pocket and the antiproliferative activity was found to correlate with Topo IIα inhibition.[26] Some α-heterocyclic thiosemicarbazones, e.g., 2-formylpyridine thiosemicarbazones, show Topo IIα inhibition activity, which is enhanced by complexation with copper(II) and formation of square-planar complexes.[27] Type II Topoisomerases are the target of a broad range of clinically used anticancer drugs.[28] The dual action mode as RNR and Topo IIα inhibitor might be a very promising strategy in fight against cancer.[29]

Since TSCs are potent chelators, a great variety of complexes has been isolated and characterized in the solid state.[30] Much less is known about the complexation behavior of TSCs in aqueous solution, especially at physiological pH.[31 –35] The generally low aqueous solubility of TSCs precluded such investigations, which are of primary importance for the understanding of the mode of action of TSCs as potential chemotherapeutics.

One of the challenges in this field is the design of novel TSCs as strong chelators and synthesis of metal complexes with enhanced aqueous solubility,[36] which are a priori oriented towards cancer specific targets.[37] Recently, we have shown that salicylaldehyde thiosemicarbazone (STSC) can be coupled to L- or D-proline (Pro) leading to conjugates with good chelating properties and improved aqueous solubility. As a result detailed studies on the stoichiometry and thermodynamic stability of iron(II), iron(III), copper(II) and zinc(II) complexes with the Pro-STSC conjugates in water/dimethyl sulfoxide (DMSO) mixture by various techniques were performed and data obtained were compared with those of the reference compound STSC.[32,33] These Pro-STSC conjugates showed moderate cytotoxic potency with IC_{50} values of 62 and 75 μM, respectively, in ovarian carcinoma CH1 cells and >100 μM in colon carcinoma SW480 cells. However, their coordination to copper(II) resulted in a 5- to 13-fold increase in

cytotoxicity in CH1 cells, based on a comparison of IC_{50} values, while in SW480 cells the enhancement of the antiproliferative activity was even higher. In both tested cell lines, L-Pro-STSC as well as its copper(II) complex showed slightly stronger antiproliferative activity than the compounds with a D-Pro moiety, yielding IC_{50} values of 4.6 and 5.5 μM for [Cu(L-Pro-STSC)Cl]Cl in CH1 and SW480 cells, respectively.[32] These results, which are very encouraging, prompted us to explore this approach further by coupling 2-formylpyridine thiosemicarbazones (FTSCs), which are known to show cytotoxicity in the nanomolar concentration range,[15,38,39] to L- or D-proline and to study the effect of this structural variation on aqueous solubility, coordination behavior, thermodynamic stability of metal complexes, cytotoxicity and Topo IIα inhibition properties in comparison to those of L- and D-Pro-STSC.

Herein we report on the synthesis, spectroscopic characterization and evaluation of the biological activity of two enantiomerically pure L- and D-proline-2-formylpyridine thiosemicarbazone (FTSC) conjugates with excellent aqueous solubility, namely 3-methyl-(*S*)-pyrrolidine-2-carboxylate-2-formylpyridine thiosemicarbazone (L-Pro-FTSC or (*S*)-H_2L) and 3-methyl-(*R*)-pyrrolidine-2-carboxylate-2-formylpyridine thiosemicarbazone (D-Pro-FTSC or (*R*)-H_2L) and their copper(II) complexes. In addition, solution equilibrium studies of the complexation of L-Pro-FTSC with copper(II) in aqueous solution have been performed by pH-potentiometry, UV−vis spectrophotometry, EPR, ^{1}H NMR, circular dichroism (CD) spectroscopy and spectrofluorometry. Speciation was also investigated in 30% (w/w) DMSO/H_2O solvent mixture for comparison. Antiproliferative activity was studied in two human cancer cell lines and Topoisomerase IIα inhibition was evaluated for both ligands and their corresponding copper(II) complexes in a DNA plasmid relaxation assay.

Results and Discussion

Synthesis and characterization of chiral thiosemicarbazones. The chiral thiosemicarbazone-proline conjugates have been prepared in six steps as shown in Scheme 1. First 6-chloromethylpyridine-2-carboxaldehyde C was synthesized in two steps starting from 2,6-dihydroxymethylpyridine A according to published procedures.[40] To prevent the aldehyde from the nucleophilic attack of the proline methylester, the aldehyde group was protected by using a standard procedure.[41] The reaction of D with L- and D-proline methylester gave E in good yield (84% for the L- and 61% for the D-enantiomer) by following a slightly modified literature protocol.[32] Deprotection of the aldehyde and the hydrolysis of

the methyl ester function with formation of F have been accomplished in water in a quantitative yield.[42] The use of dry ethanol was crucial for the isolation of thiosemicarbazone-proline conjugates H_2L resulted from condensation of the aldehyde F with thiosemicarbazide, because this highly hydrophilic product does not precipitate in wet ethanol. One dimensional ^1H and ^{13}C NMR and two dimensional ^1H-^1H COSY, ^1H-^1H TOCSY, ^1H-^1H NOESY, ^1H-^{13}C HSQC and ^1H-^{13}C HMBC NMR spectra were in agreement with the expected structure, enabling the assignment of all ^1H and ^{13}C resonances. The purity of these compounds was further confirmed by elemental analyses. The ESI mass spectra recorded in a positive ion mode showed a strong peak at *m/z* 308 due to the $[M + H]^+$ ion. The results of the pH-metric titrations (vide infra) suggest that L-Pro-FTSC is tribasic in the studied pH-range and adopts a zwitterionic structure as shown in Scheme 1.

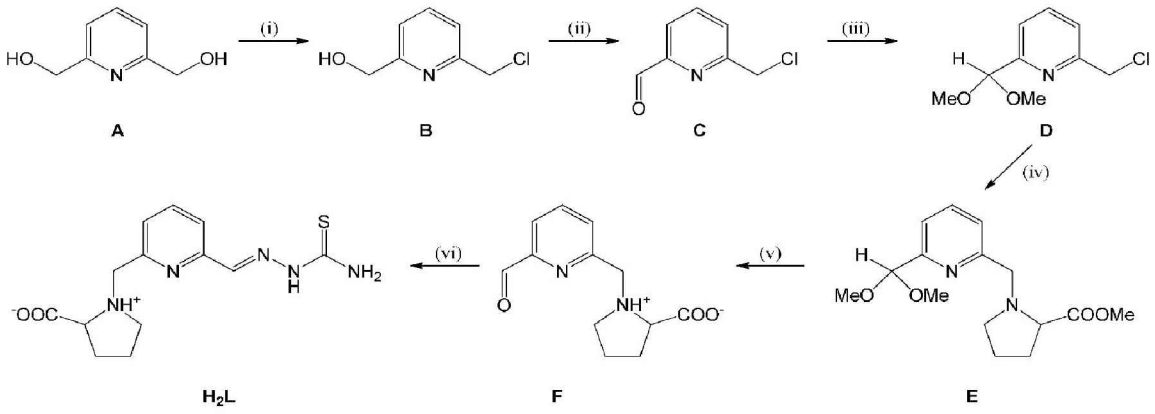

Scheme 1. Synthesis of chiral thiosemicarbazone-proline derivatives (*S*)-H_2L and (*R*)-H_2L.[a]

[a]Reagents and conditions: (i) and (ii) see ref. 41; (iii) trimethyl orthoformate, methanesulfonic acid, methanol, 78 °C, 3 h; (iv) L- or D-proline methylester hydrochloride, triethylamine, THF/CH_2Cl_2 1.5:1, 40 °C, 12 h, purification by column chromatography; (v) water, reflux, 48 h; (vi) thiosemicarbazide, EtOH abs. 78 °C, 24 h.

Synthesis and characterization of the copper(II) complexes. By the reaction of copper(II) acetate monohydrate with both proline – thiosemicarbazone conjugates in water the two complexes [Cu(*S,R*)-L] and [Cu(*R,S*)-L] have been isolated in 70 and 55% yield, respectively. Strong peaks at *m/z* 391 and *m/z*

369 were attributed to $[M + Na]^+$ and $[M + H]^+$ respectively in the ESI mass spectra recorded in a positive ion mode. The structure of [Cu(*S*,*R*)-L] was also established by X-ray diffraction.

X-ray Crystallography. The result of X-ray diffraction study of [Cu(*S*,*R*)-L]·2H_2O is shown in Figure 1. The complex crystallizes in the noncentrosymmetric orthorhombic space group $P2_12_12_1$ with one molecule of the complex and two water molecules in the asymmetric unit. The copper(II) complex has a square-pyramidal coordination geometry (τ parameter is 0). The ligand acts as a pentadentate doubly-deprotonated one, binding to copper(II) via pyridine nitrogen N1, imine nitrogen N2, thiolato atom S, tertiary nitrogen N5, and carboxylato oxygen O1. Upon coordination of L-prolinate moiety to copper(II) via the nitrogen atom N5 the latter, in addition to C12, becomes a chiral center. The literature data[43] show that in most cases the nitrogen atom adopts the same configuration as the asymmetric prolinate carbon. In rare cases, however, the nitrogen and the asymmetric carbon of the proline moiety adopt opposite configurations by coordination to metal or protonation of the nitrogen atom.[44] In [Cu(*S*,*R*)-L]·2H_2O the atoms C12 and N5 adopt opposite configurations, namely S_CR_N. A salient feature is the formation of four five-membered chelate cycles upon coordination of the ligand to copper(II). Three of them are essentially planar, while the fourth prolinic moiety adopts a half-chair conformation.

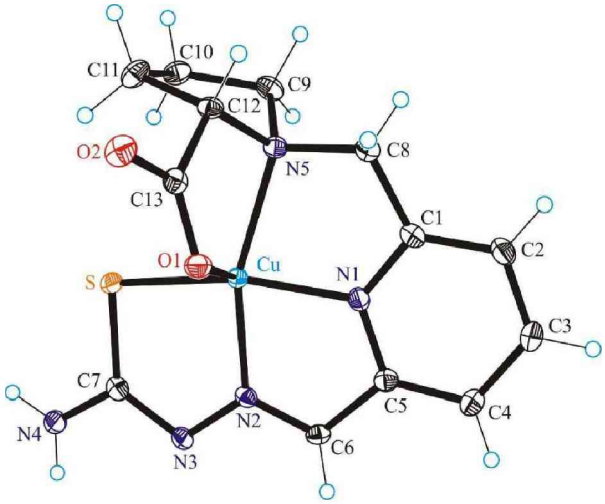

Figure 1. ORTEP view of [Cu(S_C,R_N)-L] with thermal displacement ellipsoids drawn at the 50% probability level. Selected bond distances (Å) and bond angles (deg): Cu–N1 1.9443(14), Cu–N2 1.9887(15), Cu–S 2.2741(4), Cu–N5 2.1312(14), Cu–O1 2.2519(13), N2–N3 1.367(2), C7–S 1.7527(19); N1–Cu–N2 79.82(6), N1–Cu–N5 81.38(6), N5–Cu–O1 76.08(5), N1–Cu–O1 96.04(6), N2–Cu–O1 113.54(5), S–Cu–O1 101.46(4).

The complex is involved in intermolecular hydrogen bonding interactions as shown in Figure S1. The nitrogen atom N4 of the terminal amino group acts as proton donor in hydrogen bonds to oxygen atom O4 of the water molecule and carboxylate oxygen atom $O1^{i}$ of the adjacent complex, while the hydrazinic nitrogen N3 and carboxylate oxygen O2 are proton acceptors in strong hydrogen bonds with O3 and $O3^{i}$ of neighboring water molecules, (atoms marked with i have been generated via symmetry transformation $x - 0.5, -y + 1.5, -z + 1$).

Solution Chemistry

Aqueous solutions of [Cu(*S,R*)-L] and [Cu(*R,S*)-L] at physiological pH are found to be optically active and both enantiomers show Cotton effects (see Figure S2 in the SI). As expected, they are roughly mirror images over the 230−380 nm region of the circular dichroism (CD) spectra, while their UV−vis spectra are identical.

Proton dissociation processes and lipophilicity of the ligand L-Pro-FTSC. Proton dissociation processes of L-Pro-FTSC were followed by pH-potentiometry, UV–vis spectrophotometry and spectrofluorometry, as well as ^{1}H NMR titrations in aqueous solution. The hydrolytic stability of the ligand was checked by consecutive pH-potentiometric titrations which showed that no ligand decomposition occurred in the pH range studied (pH 2.0−11.5) under the argon atmosphere. Although, this ligand consists of four functional groups (COOH, $N_{Pro}H^{+}$, $N_{pyr}H^{+}$ and $N_{hydrazinic}H$, see Scheme 1), which presumably dissociate, only three proton dissociation constants could be determined (Table 1) in the pH range studied. Based on the pK_a values of structurally similar TSCs, such as FTSC and L-Pro-STSC),[32,34] low pK_a values are expected for the COOH and $N_{pyr}H^{+}$ moieties, while significantly higher values for the $N_{Pro}H^{+}$ and $N_{hydrazinic}H$ functionalities. pK_a values were measured in 30% (w/w) DMSO/H_2O solvent mixture as well, and found to be comparable to those obtained in neat water. However, pK_1 is slightly and pK_3 is markedly higher in the presence of DMSO (Table 1). These changes indicate proton dissociation of neutral functional groups such as COOH (pK_1) and $N_{hydrazinic}H$ (pK_3). At the same time pK_2 shows practically no solvent-dependent change suggesting an isoelectronic deprotonation process such as $N_{Pro}H^{+} \rightleftharpoons N_{Pro} + H^{+}$. The proton dissociation steps of L-Pro-FTSC were assigned to the different functional groups by the careful analysis of the results of the UV–vis and ^{1}H NMR titrations. The pH-dependent UV–vis spectra recorded between pH 2.0 and 11.5 show

characteristic spectral changes at pH < ~2.5 and pH > ~9.5, while spectra remain unchanged in the middle pH range (Figure 2A,B).

Table 1. Proton dissociation constants (pK_a) of the ligand L-Pro-FTSC determined by various methods[a] {T = 298 K, I = 0.10 M (KCl)}.

	pH-metry	UV−vis	^{1}H NMR
pK_1	1.86(2); 2.13(2)[b]	–	–
pK_2	8.78(2); 8.74(2)[b]	–	8.84(2)
pK_3	11.08(2); 11.43(1)[b]	11.03(1)	11.04(1)

[a] The numbers in parentheses are standard uncertainties of the quoted pK_a values. [b] Determined in 30% (w/w) DMSO/H_2O

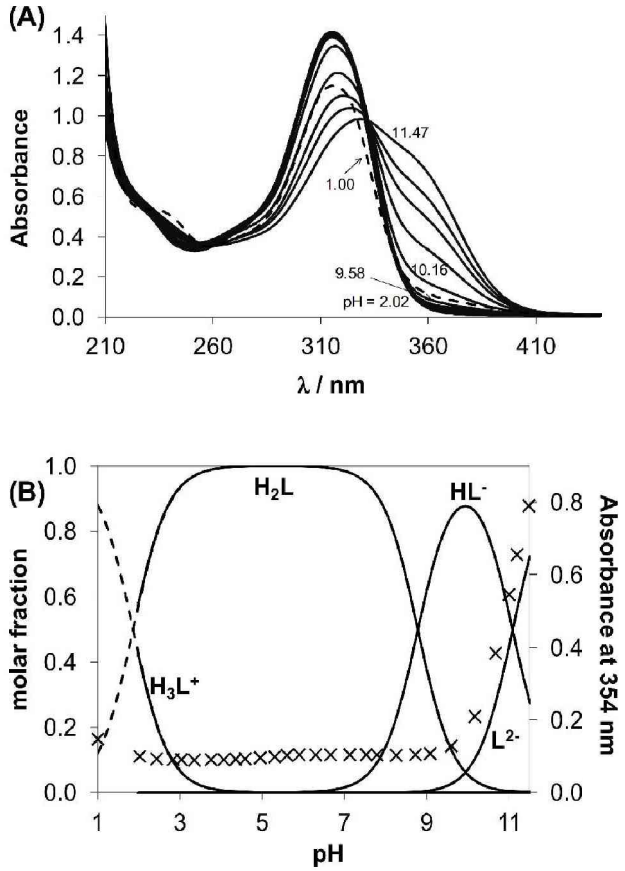

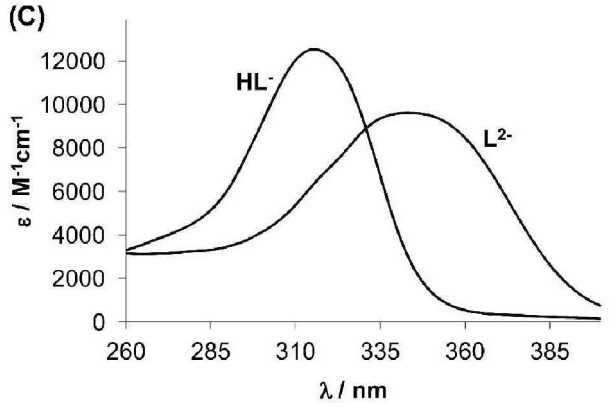

Figure 2. UV–vis absorbance spectra of L-Pro-FTSC recorded in the pH range of 2.0 − 11.5 (solid lines) and at pH 1.00 (dashed line) (c_L = 0.113 mM; T = 298 K; I = 0.10 M (KCl); l = 1 cm) (A); Concentration distribution curves for ligand species with the pH-dependence of absorbance values at 354 nm (×) (B); Molar absorption spectra of the individual ligand species (HL^-, L^{2-}) (C).

The deprotonation of the COOH (and $N_{Pro}H^+$ in the basic pH range) are not expected to be accompanied by significant spectral changes, unlike $N_{pyr}H^+$ and hydrazinic-NH. Spectra recorded at pH < ~2.5 showing some changes suggest that the $N_{pyr}H^+$ deprotonates along with COOH. On the other hand the $N_{hydrazinic}H$ of the thiosemicarbazide moiety releases most probably the proton at pH > ~9.5, and the negative charge is mainly localized on the S atom via thione/thiol tautomeric equilibrium. It is worth noting that the individual molar absorbance spectra of the HL^- and L^{2-} forms (Figure 2C) show strong similarity with the spectra of the corresponding species of FTSC considering the λ_{max} values and the position of the isosbestic point.[34] Besides the individual spectra of the ligand species (HL^- and L^{2-}), pK_3 value was also calculated on the basis of the deconvolution of the spectra recorded (Table 1). Good agreement with the data obtained from the pH-potentiometric data should be mentioned.

The pH-dependent ^{1}H NMR spectra of the ligand (Figure 3) revealed that certain proton resonances are quite sensitive to stepwise deprotonation (Figure S3 in the SI). Namely, the first deprotonation step results in small changes of the chemical shifts (δ) of the C^8H of the Pro moiety, as well as $C^{13}H$=N, and the pyridine ring protons, suggesting the concurrent deprotonation of $N_{pyr}H^+$ and COOH at pH < ~ 2.5. The second deprotonation is also accompanied by significant electronic shielding effects, such as the upfield shift of the $C^{13}H$=N, $C^4H_{(Ar)}$ and the proline ring CH_2, C^7H_2 and C^8H protons, while the signal of

the $C^6H_{(Ar)}$ proton remains intact. Further changes were observed at pH > ~10 due to the third deprotonation step, especially in the case of the $C^{13}H$=N proton signal showing a considerable downfield shift upon increasing the pH, while the position of the peaks of the proline ring CH_2, C^7H_2 and C^8H protons remains unaltered. Based on the shift of the position of the $C^{13}H$=N, $C^6H_{(Ar)}$ protons, pK_2 and pK_3 have been calculated. The values obtained correspond well to those resulted from the other methods (Table 1).

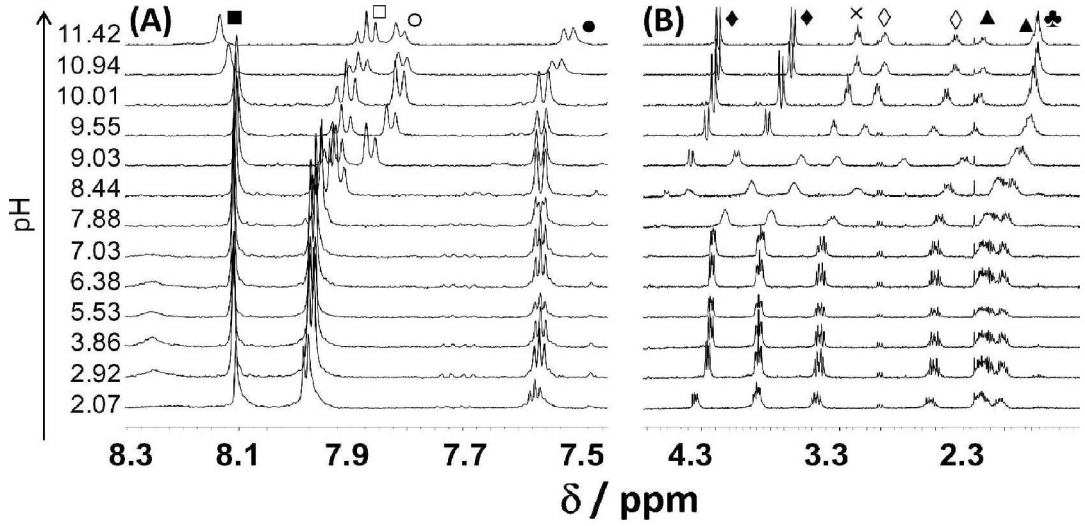

Figure 3. Low- (a) and high-field (b) regions of the ^{1}H NMR spectra of the L-Pro-FTSC at different pH values (c_L = 1.0 mM; T = 298 K; I = 0.10 M (KCl); 10% D_2O). *Symbols:* ●: $C^6H_{(Ar)}$; ○: $C^4H_{(Ar)}$; □: $C^5H_{(Ar)}$; ■: $C^{13}H$=N; ♦: C^7H_2; ×: C^8H; ◊: $C^{11}H_2$; ▲: C^9H_2; ♣: $C^{10}H_2$.

Note that the C^7H_2 protons are displayed in ^{1}H NMR spectra as two doublets because of the non-equivalent orientation in space of the two protons. On the other hand the peaks belonging to $C^4H_{(Ar)}$ and the proline ring CH_2 protons appear in two sets at pH < ~7.5 most probable due to the presence of *Z* and *E* isomers of the ligand and slow isomerization processes with respect to the NMR time scale ($t_{1/2}$(obs) > ~1 ms). These peaks start to broaden at pH > ~7.5 up to pH ~ 9 and only one set of signals is seen at pH > ~9 owing to the faster isomerization or the presence of only one kind of isomer.

The results of the UV–vis and ^{1}H NMR titrations indicate that the COOH group and $N_{pyr}H^+$ have quite low pK_a values (pK_a << 2) and can be considered deprotonated at pH < 3. pK_1, pK_2 and pK_3 most probably belong to the deprotonation of COOH (partly overlapped with the deprotonation of $N_{pyr}H^+$), $N_{Pro}H^+$ and the hydrazinic-NH, respectively (Scheme 2). In addition, the pK_a values of the initial aldehyde F in Scheme 1 were determined in neat water (pK_1 = 2.19(4) and pK_2 = 8.91(2)). These can be attributed to the deprotonation of the COOH (overlapped with that of $N_{pyr}H^+$) and $N_{Pro}H^+$ moieties, respectively. Due to the lack of the hydrazinic-NH in this aldehyde, these data provide unequivocal evidence that the pK_3 of L-Pro-FTSC belongs to the deprotonation of hydrazinic-NH.

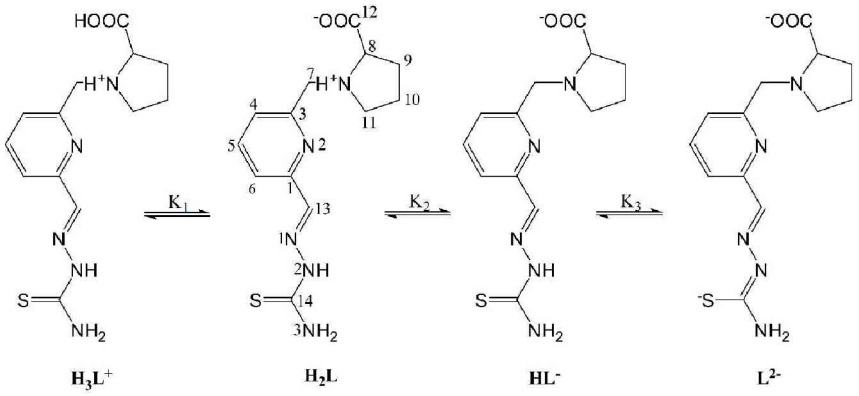

Scheme 2. Deprotonation steps of H_3L^+ (relevant for both Pro-FTSC enantiomers). In the first step deprotonation of $N_{pyr}H^+$ does overlap with that of COOH.

L-Pro-FTSC possesses intrinsic fluorescence due to its extended conjugated electronic structure (see Figure S4 in the SI). The fluorescence emission increases with increasing pH reaching a maximum at pH ~ 7.5, while the second and third deprotonation steps are accompanied by decrease of the emission intensity (see Figures S4B in the SI).

The hydrophilic character of the ligands L- and D-Pro-FTSC was studied at pH 7.4 via the partitioning between *n*-octanol and water. The ligands were found to be very hydrophilic and practically no ligand could be detected in the organic phase after partitioning. Therefore, only a threshold limit could be estimated for the distribution coefficients (D) of the ligands, thus log$D_{7.4}$ < −1.7. This low log$D_{7.4}$ value

is manifested in enhanced aqueous solubility compared to other chemically related TSCs, such as L- and D-Pro-STSC ($\log D_{7.4}$ = −0.56 (L), −0.60 (D)),[32] or Triapine ($\log D_{7.4}$= +0.85),[33] which allowed us to perform the equilibrium studies in neat water. At physiological pH the L-Pro-FTSC ligand is mainly present in its neutral form (96% H_2L, 4% HL^-; see Figure 2B), but adopts a zwitterionic structure.

The lipophilicity of the copper(II) complexes of both ligands was also studied at physiological pH, but their strong hydrophilic character did not allow the accurate determination of the $\log D_{7.4}$ values ($\log D_{7.4}$ < −1.7).

Complexation reactions of copper(II) with L-Pro-FTSC. The complex formation processes were studied primarily by pH-potentiometry in water. The proton displacement by the metal ion due to the complex formation is almost complete already at the starting pH value (pH ~2), indicating the high stability of the copper(II) complexes formed with L-Pro-FTSC. The stoichiometries and the cumulative stability constants of the metal complexes furnishing the best fits to the experimental data are listed in Table 2. The stability constant of the species $[CuLH]^+$ was determined by UV−vis spectrophotometry on individual samples in which the KCl was partially or completely replaced by HCl to maintain the ionic strength constant in the pH range 0.9 – 2.0, and the changes of the metal-to-ligand charge-transfer (CT) bands were followed (Figure 4). Then the determined $\log\beta$ of $[CuLH]^+$ was kept constant during the pH-potentiometric data evaluation. Data in Table 2 reveal that copper(II) forms merely mono-ligand complexes with L-Pro-FTSC and there was no indication for the formation of bis-ligand complexes.

Table 2. Cumulative stability constants ($\log\beta$ ($M_pL_qH_r$)) of the copper(II) − *L*-Pro-FTSC complexes in water and in 30% (w/w) DMSO/H_2O[a] {T = 298 K, I = 0.10 M (KCl)}.

	$[CuLH]^+$	$[CuL]$	$[CuLH_{-1}]^-$	pM[b]
H_2O	24.03(3)[c]	21.64(1)	9.59(4)	17.5
30% (w/w) DMSO/H_2O	24.80(2)[c]	22.85(2)	10.03(9)	18.4

[a] The numbers in parentheses are standard uncertainties of the quoted $\log\beta$ values determined by pH-potentiometry. [b] pM = −log[M] at pH 7.40; c_L/c_M = 10; c_M = 0.001 mM. [c] Determined by UV−vis spectrophotometry from spectra recorded at pH 0.9−2.0.

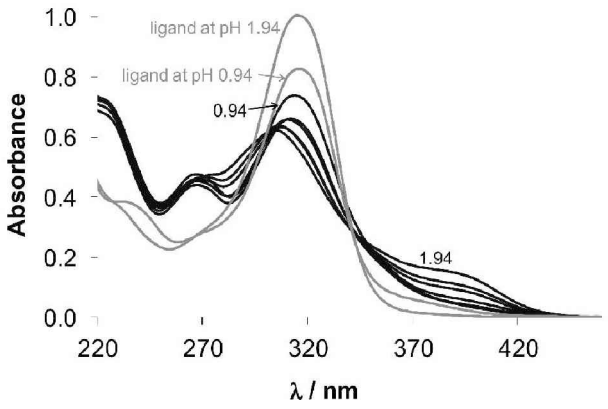

Figure 4. UV–vis absorbance spectra of copper(II) – L-Pro-FTSC system recorded in the pH range 0.94 – 1.94 (c_L = 0.042 mM; M:L = 1:1; T = 298 K; I = 0.10 M (KCl); l = 1 cm).

Complexation of copper(II) with L-Pro-FTSC was also studied in a 30% (w/w) DMSO/H_2O solvent mixture for comparison, since this medium was applied for metal ion – TSC systems in our previous works, where the ligands and their complexes exhibited much lower aqueous solubility.[32–] The speciation of copper(II) – L-Pro-FTSC complexes in the presence of the 30% (w/w) DMSO was found to be quite similar, but not identical with that in neat water (Table 2, Figure 5).

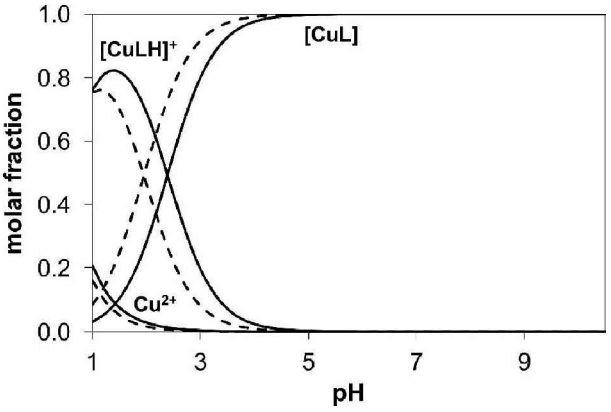

Figure 5. Concentration distribution curves of the copper(II) – *L*-Pro-FTSC system in water (solid lines) and in 30% (w/w) DMSO/H_2O mixture (dashed lines) (c_L = 1.0 mM; M:L = 1:1; T = 298 K; I = 0.10 M (KCl)).

In order to compare the stability of the copper(II) complexes of L-Pro-FTSC with other metal thiosemicarbazonates at physiological pH, pM values have been computed (Table 2). The higher pM value indicates stronger chelating ability. pM stands for the negative logarithm of the equilibrium concentrations of the free metal ion under certain conditions. The pM value of the L-Pro-FTSC system is significantly higher than that of the L-Pro-STSC coordinated via the (O^-,N,S^-) donor atoms (pM = 13.4)[33] and the well-known TSC, Triapine with the (N_{pyr},N,S^-) donor set (pM = 11.6)[36] calculated under identical conditions at pH 7.40 for comparison in 30% (w/w) DMSO/H_2O. The very high stability of the [CuL] complex of L-Pro-FTSC, which predominates at physiological pH even at the submicromolar concentrations, strongly suggests the possible coordination of the functionalities of the proline moiety such as the COO^- and proline-N in solution, in addition to the N_{pyr},N,S^- donor set of thiosemicarbazide. The pentadentate (N_{pyr},N,S^-,COO^-,N_{Pro}) coordination mode of L-Pro-FTSC was also confirmed by single-crystal X-ray crystallography of the copper(II) complex (Figure 1). On the other hand in the species $[CuLH]^+$ the non-coordinating hydrazinic-N atom is most probably protonated. $[CuLH_{-1}]^-$ is a minor complex present only in the strongly alkaline medium. The formation of a mixed-hydroxido species was suggested, since the base consumption has exceeded the number of dissociable protons in the ligand.

In order to confirm the speciation obtained by the pH potentiometry and to gain information about the coordination modes of the L-Pro-FTSC in its complexes, UV−vis, EPR and CD spectroscopic measurements were performed.

UV−vis spectra for the copper(II) − L-Pro-FTSC [CuL] complex recorded in the wavelength range 450 – 800 nm (Figure S5 in the SI) display a d−d transition band which is partly overlapped with stronger S−Cu ligand-to-metal CT bands. The λ_{max} value of the d−d transition is decreased from 625 nm down to 610 nm parallel with the formation of species [CuL] from $[CuLH]^+$ upon increasing the pH from 2 to 3, and it becomes constant at pH > ~3 at 1:1 metal-to-ligand ratio. CD spectra in the wavelength range 530 – 680 nm show characteristic pH-dependent changes (Figure S6 in the SI). The location of the minima of the peaks is shifted from 721 nm to 685 nm by increasing the pH up to ~3, but no more significant changes were observed by further increase of the pH.

EPR spectra of copper(II) – L-Pro-FTSC species in aqueous phase were recorded at various pH values at room temperature (Figure 6) and at 77 K (Figure S7 in the SI). They confirm the speciation obtained by the pH-potentiometry and reveal the coordination mode of the ligand in each copper(II) complex. The fitted experimental and individual spectra are depicted in Figure 6. A simulation of the solution EPR spectra resulted in the individual isotropic EPR parameters of complexes $[CuLH]^+$ and [CuL] (Table 3). The coordination of three non-equivalent nitrogen atoms can be unequivocally supported for both complexes. Although the nitrogen splitting is not fully resolved, the line shape was still indicative and the spectra could be fitted with a higher regression coefficient (R = 0.9954) by assuming three nitrogen donor groups instead of only two (R = 0.9933). Furthermore the low g_o values suggest the involvement of the thiolato (S^-) group into the coordination. The formation constants obtained by the "two-dimensional" simulation of the EPR spectra are in good agreement with the pH-potentiometric results (cf. Tables 2 and 3).

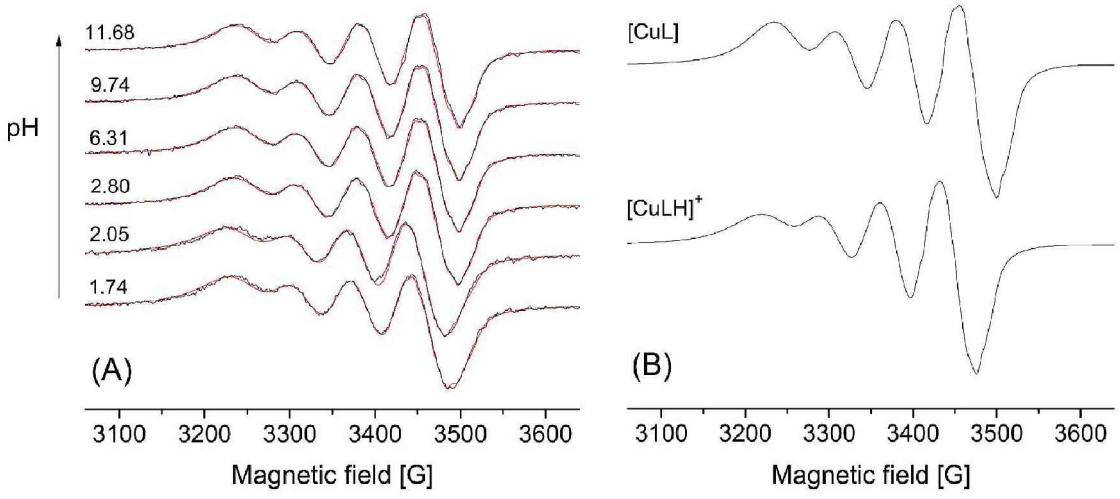

Figure 6. Experimental (black trace) and simulated (red trace) EPR spectra recorded for the copper(II) – L-Pro-FTSC system in water (A); Calculated component EPR spectra obtained for copper(II) – L-Pro-FTSC complexes (B) (c_L = 1.0 mM; M:L = 1:1; T = 298 K; I = 0.10 M (KCl)).

The frozen solution EPR spectra of complex $[CuLH]^+$ recorded in strongly acidic medium, could be fitted by assuming the usual elongated octahedral geometry of copper(II) complexes. However, axial symmetry of the *g*- and *A*-tensors was not sufficient, and rhombic symmetry has been taken into account. The largest nitrogen hyperfine coupling of the three non-equivalent nitrogen atoms could be determined from the simulation of superhyperfine structure well-resolved in the perpendicular range of the spectra (3200 – 3400 G in Figure 7A). These data also support the pentadentate (N_{Pro},N_{pyr},N,S^-,COO^-(axial)) nature of the ligand in [CuL] with a square-pyramidal coordination geometry established by X-ray diffraction. The frozen solution EPR spectra of [CuL] indicated a surprisingly different structure of the complex compared to that at room temperature. At 77 K the predominant formation of a dimeric $[Cu_2L_2]$ species could be detected. The half-field peak, measured at 1650 G, can be attributed to a double quantum transition ($\Delta M_S = 2$) of a coupled spin system, established by two neighboring copper(II) centres (Figure S7). The EPR spectra of the dimeric species are usually characterized by assuming a zero-field splitting in a triplet state with $S = 1$, and the axial (D) and rhombic (E) parameter of zero-field splitting is determined.[45] This approximation can give reliable results, when the exchange coupling is much stronger than the copper hyperfine coupling ($J > 5\times A^{Cu}$). However, some features of the spectra cannot be described by this assumption. This is the case when the exchange interaction is in the order of magnitude of the copper hyperfine coupling ($J \sim A$). The exact solution of the Hamiltonian would solve these problems, although there are only few examples for the use of this possibility.[46] Furthermore, the exact description of a coupled spin system can result in effective structural parameters, including the copper(II)-copper(II) distance and the orientation of the two *g*-tensors relative to each other, based on which the structure of a dimeric species can be proposed. The EPR spectra measured at pH > ~ 5 could be simulated by the complete diagonalization of the Hamiltonian of a two-spin system by the "EPR" program. (For program description see section "EPR measurements and deconvolution of the spectra" in the Experimental part). These measured spectra were described by the superposition of a dimeric and a monomeric species in a ratio of 92% to 8%, respectively (Figure 7).

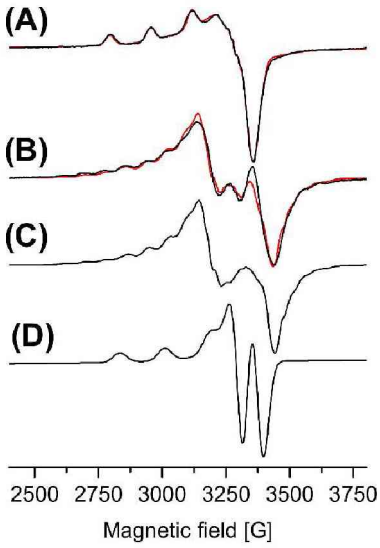

Figure 7. Experimental (black trace) and simulated (red trace) EPR spectra recorded at (c_L = 1.0 mM; M:L = 1:1; T = 77 K; I = 0.10 M (KCl) (A) pH = 2.0 and (B) pH = 5.3; Spectrum (B) was simulated by the superposition of the dimeric component (C) with 92% abundance and the monomeric component (D) (8% abundance). EPR parameters of (C) are g_x = 2.036, g_y = 2.060, g_z = 2.175, A_x = 7.1 G, A_y = 18.2 G, A_z = 180.0 G copper(II) hyperfine coupling, D = 175.0 G dipolar coupling, J > 1500 G spin-exchange coupling $\chi = 30^o$ and $\psi = -55^o$ polar angles, and $\alpha = 0^o$, $\beta = 3.8^o$, $\gamma = 5.5^o$ Euler angles. Calculated EPR parameters of spectrum (A) and (D) are listed in Table 3.

The complex $[Cu_2L_2]$ could be simulated assuming two identical copper(II) centres with almost parallel equatorial plane (all three Euler angles are close to zero), with polar angles of $\chi = 31^o$, $\psi = 55^o$, and dipolar coupling D = 175.0 G (Figure 7B and C). For the exchange coupling we can give the estimation of J > 1500 G, as under this value a doublet peak originated from this interaction should have been detected under the experimental conditions. From the dipolar coupling the copper(II)-copper(II) distance of 6.8 Å could be calculated by using the point dipole approach. The very small g_z value of 2.175 and large A_z = 180 G suggest high ligand field around the copper(II) centres. A possible structure in accordance with the above structural data is depicted in Figure 8.

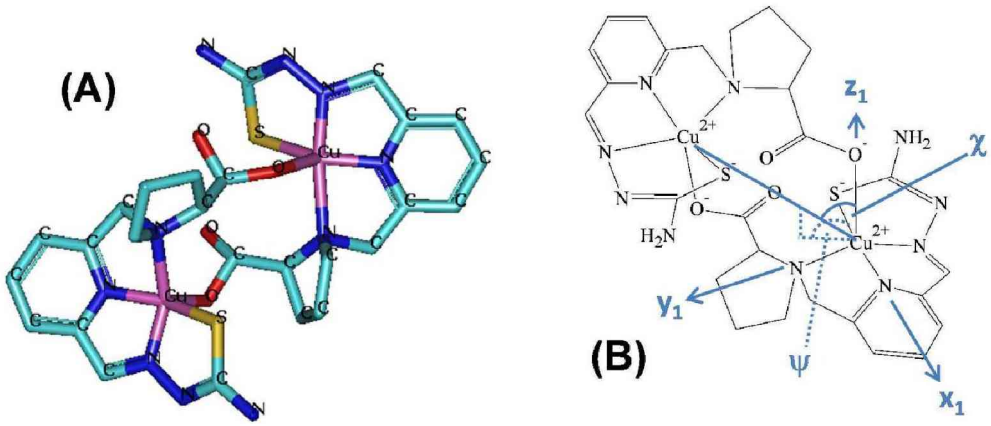

Figure 8. Proposed structure of $[Cu_2L_2]$ dimeric complex detected in the frozen solution of copper(II) – L-Pro-FTSC system; (A) 3D structure obtained by molecular mechanics optimization; (B) schematic structure showing the *g*-tensor orientations and the (χ,ψ) polar angles used in the EPR spectrum simulation.

Table 3. EPR parameters and stability constants of the components obtained for copper(II) – L-Pro-FTSC complexes

	Logβ [a]	**Isotropic EPR parameters**[a]			**Anisotropic EPR parameters**[b]			**Calculated isotropic EPR parameters**[c]	
		g_o	A_o [G]	a^N_o [G]	g_x g_y g_z	A_x [G] A_y [G] A_z [G]	a_y^{N1} [G] a_y^{N2} [G] a_x^{N3} [G]	$g_{o,calc}$	$\lvert A_{o,calc}\rvert$ [G]
$[CuLH]^+$	23.66(1)	2.1030(3)	65.1(3)	15.5(6)	2.058	−23.1	18.3	2.1040	69.3
				12.1(5)	2.035	−20.6	18.3		
				9.2(5)	2.219	−156.8	14.5		
[CuL]	21.69(1)	2.0913(1)	67.5(1)	16.9(1)	2.040	−20.1		2.0880	70.3
				12.4(1)	2.046	−8.9			
				9.0(2)	2.178	−174.9			

[a] The numbers in parentheses are standard uncertainties of the quoted values. [b] The experimental errors were ±0.001 for g_x and g_y and ±0.0005 for g_z, ± 2 G for A_x and A_y and ±1 G for A_z and ±0.5 G for a^N. [c] Isotropic values calculated via the equation $g_o = (g_x+g_y+g_z)/3$, and A_o [MHz] $= (A_x+A_y+A_z)/3$.

In this geometrically optimized structure the two identical and parallel copper(II)-copper(II) centres with the equatorial coordination of $[N_{Pro},N_{pyr},N^-,S^-]$ are connected axially by the carboxylate O^- of the proline group. The distance of 5.8 Å, and the estimated polar angles of $\chi = 49^o$, $\psi = 44^o$ are acceptably close to the simulated data. For the monomeric species, we obtained very similar principal values for the *g*- and *A*-tensors (see Table 4 and Figure 7D) as were found for the dimeric complex, which suggests that the only difference is that in the monomeric species the carboxylate O^- of the proline group coordinates axially to its own copper(II) ion (cf. Figures 1 and 8).

Stability of the copper(II) complex of L-Pro-FTSC in Minimum Essential Medium (MEM) and its interaction with HSA. MEM is usually used for the in vitro cytotoxicity studies of the metal complexes and ligands. It contains various amino acids as potential competitor ligands for the metal-containing species. To assess the stability of the [CuL] complex of L-Pro-FTSC in this medium, EPR spectra of the complex in MEM and in aqueous solution at pH 7.40 for comparison were measured (Figure S8 in the SI). The spectra of [CuL] in MEM and in water (HEPES buffer) are fairly similar providing strong evidence that the complex is stable in MEM.

Similar experiment was performed in the presence of human serum albumin (HSA). HSA is the most abundant of the human blood serum proteins occurring to the extent of 0.63 mM and it serves as a transport vehicle for a wide variety of endogenous species such as copper(II) and zinc(II) ions and exogenous compounds and various pharmaceuticals. In order to get an insight into the interaction of the [CuL] with HSA, EPR spectra were recorded at room temperature in the absence and in the presence of the protein. The spectra for the copper(II) − HSA system have been also measured for comparison, and frozen solution spectra caused by the slow motion of the copper(II) ion verified the complexation with the protein. However, in the case of [CuL] – HSA system the EPR spectrum reveals that the protein practically does not change the isotropic spectrum of [CuL] under the condition used (Figure S8 in the SI). The interaction of [CuL] with HSA was also monitored by UV−vis spectrophotometry at pH 7.40. Spectra were recorded for HSA at various concentrations in the absence or in the presence of [CuL] (Figure S9A in the SI). Displacement of the ligand by HSA would result in significant decrease of the absorbance at ~390 nm (Figure S9D) and an increase at $\lambda < 300$ nm due to the binding of the copper(II)

ion to HSA (Figure S9C in the SI). When no interaction takes place between the metal complex and the protein the spectrum for the [CuL] – HSA system would be the sum of the spectra of [CuL] and HSA measured separately. This was the case for the [CuL] – HSA system, indicating that there was no marked interaction between the complex and HSA even at 10-fold excess of the protein (Figure S9B in the SI).

Cytotoxicity in Cancer Cell Lines

Antiproliferative activity of (*S*)-H_2L, (*R*)-H_2L and of their corresponding copper(II) complexes [Cu(*S*,*R*)-L] and [Cu(*R*,*S*)-L] was studied by colorimetric microculture assay (MTT assay) in human ovarian carcinoma (CH1) and colon carcinoma (SW480) cell lines. IC_{50} values for the L- and D-conjugates, as well as for the copper(II) complexes in SW480 cells could not be determined within the chosen concentration range (max. concentration 300 μM). In CH1 ovarian carcinoma cells IC_{50} values of 123 ± 39 μM and 113 ± 16 μM were obtained for the copper(II) complexes [Cu(*S*,*R*)-L] and [Cu(*R*,*S*)-L], respectively. However, the free ligands showed a markedly reduced activity in CH1 cells. The corresponding concentration-effect curves in CH1 cells are shown in Figure 9. The found IC_{50} values for both complexes are remarkably lower than for the recently reported L- and D-proline thiosemicarbazone conjugates based on 2-hydroxybenzaldehyde showing values in the low micromolar concentration range. Nevertheless, our results are in good accordance with those recently published by us, which have shown enhanced antiproliferative effects of the copper(II) complexes compared to their corresponding ligands.[33]Although, both ligands display a reduced activity they are characterized by an excellent solubility in water and complete culture medium, which is a major advantage compared to several previously evaluated thiosemicarbazones, e.g., Triapine. Moreover, the enhanced aqueous solubility is a premise for further biological evaluation *in vivo,* where a good solubility in biocompatible media is required.

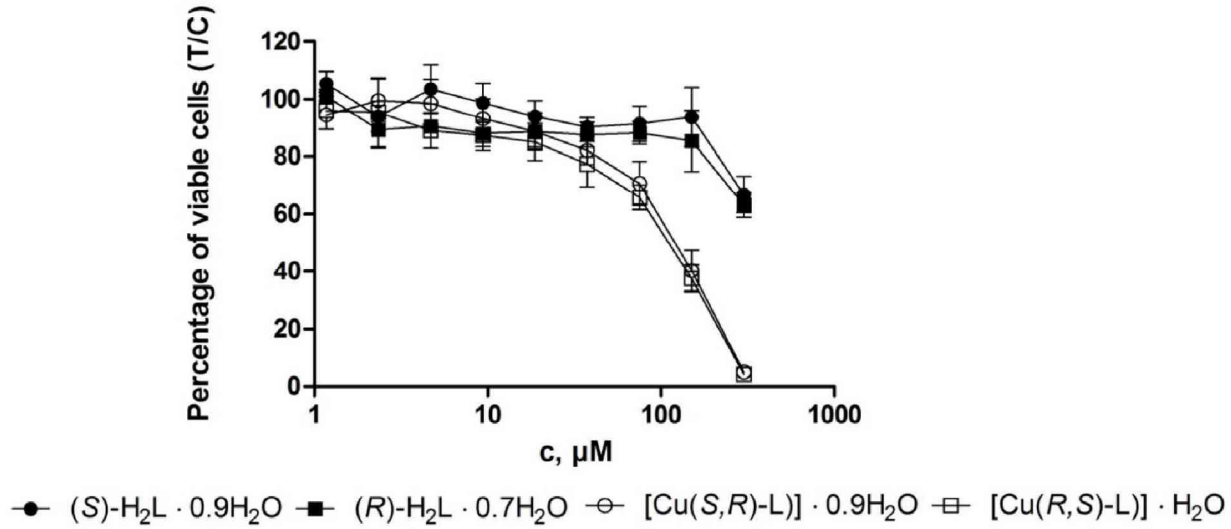

Figure 9. Concentration-effect curves of (*S*)-H_2L and (*R*)-H_2L and their corresponding copper(II) complexes [Cu(*S*,*R*)-L] and [Cu(*R*,*S*)-L] in CH1 ovarian cancer cells were obtained by MTT assay (96 h exposure).

Topoisomerase IIα inhibition capacity

We investigated the Topo IIα inhibition activity for the L- and D- proline thiosemicarbazone conjugates and their corresponding copper(II) complexes. The inhibition of Topo IIα showed a clear correlation with the cytotoxic properties of the compounds. The complexes [Cu(*S*,*R*)-L] and [Cu(*R*,*S*)-L] displayed a high capacity of inhibiting this enzyme in the cell free DNA plasmid relaxation assay at a concentration of 300 μM, however, they did not show significant inhibition of the enzyme activity at a concentration of 50 μM (Figure 10). In contrast, the ligands L-Pro-FTSC and D-Pro-FTSC did not inhibit the enzyme appreciably at all used concentrations. Concurrent studies proved that Cu^{2+} is not capable of inhibiting the Topo IIα activity at concentrations up to 500 μM.[27] Hence, a significantly higher Topo IIα inhibition ability of the copper(II) complexes is obvious. Our results are in good agreement with the literature. Previous studies demonstrated that heterocyclic-substituted copper(II)-thiosemicarbazonates are capable of inhibiting the Topo IIα activity by preventing the formation of the DNA-enzyme complex or by interfering with the ATP domain of the enzyme.[27,28,47,48] The results of our study suggest that Topo IIα is

an additional target for [Cu(*S*,*R*)-L] and [Cu(*R*,*S*)-L] complexes. A significantly higher inhibition capacity of the copper(II) complexes in contrast to their corresponding ligands demonstrates that the metal coordination has a considerable impact on the biological activity of these proline-thiosemicarbazone conjugates.

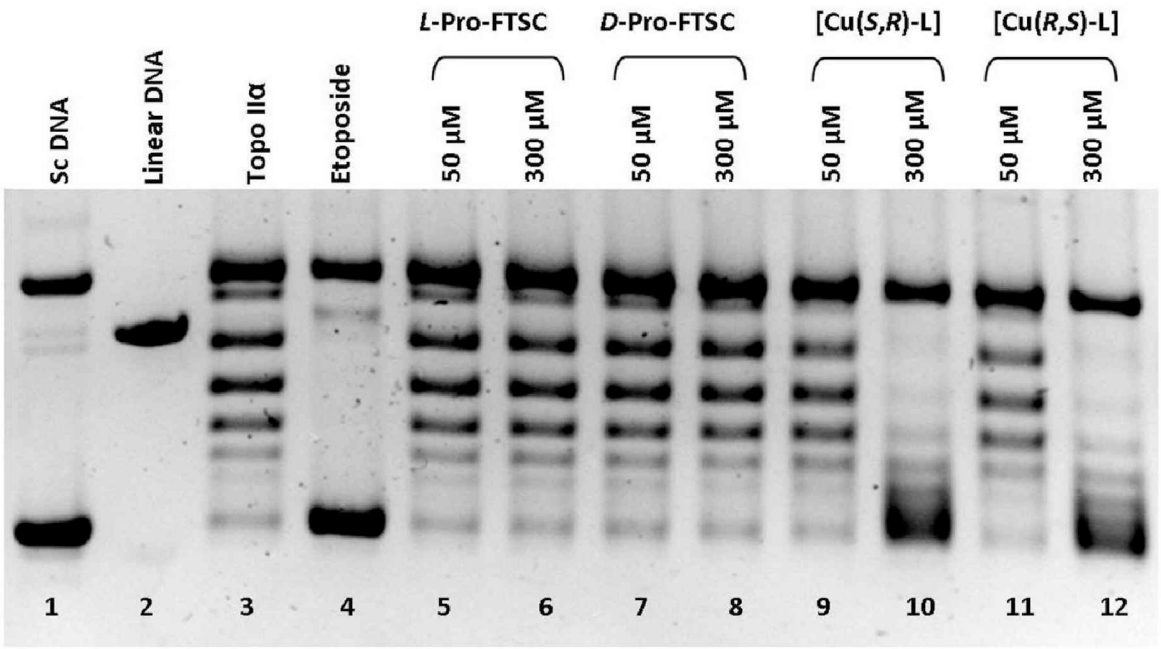

Figure 10. Topo IIα inhibition capacity of L- and D-Pro-FTSC conjugates and their corresponding copper(II) complexes was determined by the plasmid DNA relaxation assay. Supercoiled and linear DNA used as references (lane 1 and lane 2, respectively). Relaxed DNA bands (lane 3) show an intact enzyme activity. Supercoiled DNA band demonstrates the inhibition of enzyme activity with addition of 2 mM Etoposide (lane 4). Lanes 5–12 display the reaction of Topo IIα with supercoiled DNA in the presence of L- and D-Pro ligands or copper(II) complexes. Incubation time was 30 min.

Conclusion

Attachment of a proline moiety to 2-formylpyridine thiosemicarbazone resulted in conjugates with very high aqueous solubility (480 mg/mL). This permitted to study the complexation reactions of L-Pro-FTSC with copper(II) chloride in neat water. The stoichiometry and stability of the copper(II) complex

with L-Pro-FTSC was investigated by pH-potentiometry, UV–vis, EPR and ^{1}H NMR spectroscopy. UV–vis and EPR spectroscopy data indicate that L-Pro-FTSC acts in solution as a pentadentate ligand via a N_{Pro},N_{py},N,S^-,COO^-(axial) donor set, building up a square-pyramidal 1:1 complex with copper(II). This coordination mode was also confirmed by X-ray crystallography. The complex is highly stable, so that its dissociation cannot occur in the physiological pH-range even at micromolar concentration, which is relevant for biological studies. In addition they remain unaltered in MEM and in the presence of HSA. These copper(II) complexes inhibit Topo IIα activity and CH1 tumor cell viability leading to cell death. Their inhibitory potential in combination with excellent water-solubility is a sound basis for further development of anticancer copper(II) thiosemicarbazonates with high Topo IIα inhibitory activity. By shifting the hydrophilic/lipophilic balance towards higher log *D* values we expect to improve the cell uptake and increase the antiproliferative activity. Complexation to metal ions which favor square-planar coordination environment, e.g. Ni(II), Pd(II) or Pt(II), can, in principle, lead to enhanced Topo IIα inhibitory activity. This work is underway in our laboratory and will be reported in due course.

Experimental

Chemicals. 2,6-Dihydroxymethylpyridine and L-proline methylester hydrochloride were purchased from Alfa Aesar, while D-proline methylester hydrochloride from Acros Organics. Solvents were dried using standard pocedures if needed.[49] 2-Hydroxymethyl-6-chloromethylpyridine and 6-chloromethylpyridine-2-carboxaldehyde were synthesized according to published procedures.[40] $CuCl_2$ (puriss, Reanal) was dissolved in known amount of HCl in order to get the copper(II) stock solution. Its concentration was determined by complexometry via the EDTA complexes.

Synthesis of ligands

2-(chloromethyl)-6-(dimethoxymethyl)pyridine. A solution of 6-chloromethylpyridine-2-carboxaldehyde (1.70 g, 10.9 mmol), trimethyl orthoformate (4.70 mL, 43.0 mmol) and methanesulfonic acid (17.7 μL, 0.27 mmol) in dry methanol (17 mL) was heated at 78 °C for 3 h (in a 100 mL Schlenk tube). The solvent was removed under reduced pressure and the residue was dissolved in $CHCl_3$ (40 mL). The solution was washed with saturated aqueous $NaHCO_3$ solution and brine, and then dried over $MgSO_4$. The solvent was removed under reduced pressure to yield a slightly yellow oil. Yield:

2.14 g, 97%. ^{1}H NMR (500 MHz, $CDCl_3$): δ 7.77 (t, J = 7.8 Hz, 1H, $C^5H_{(Ar)}$), 7.51–7.47 (m, 2H, $C^4H_{(Ar)}$, $C^6H_{(Ar)}$), 5.35 (s, 1H, $CH(OMe)_2$), 4.71 (s, 2H, CH_2Cl), 3.41 (s, 6H, $(OCH_3)_2$).

(*S*)-methyl-1-(dimethoxymethyl)pyridin-2-yl-methyl-pyrrolidine-2-carboxylate. A solution of L-proline methylester hydrochloride (2.41 g, 14.55 mmol) in CH_2Cl_2 (48 mL) was treated with triethylamine (4.45 mL, 32.1 mmol) in THF (13 mL) and then combined with a solution of protected aldehyde (1.96 g, 9.7 mmol) in THF (48 mL). The reaction mixture was heated at 40 °C overnight. The white precipitate of triethylammonium chloride was filtered off to give a slightly yellow clear solution, which was freed from solvent under reduced pressure. The oily residue was purified by column chromatography using a mixture of $CHCl_3$:MeOH 97.5:2.5 as eluent. The product was obtained after removal of the solvent as a slightly yellow oil. Yield: 2.41 g, 84%. ^{1}H NMR (500 MHz, $CDCl_3$): δ 7.69 (t, J = 7.7 Hz, 1H, $C^5H_{(Ar)}$), 7.46 (d, J = 7.0 Hz, 1H, $C^6H_{(Ar)}$), 7.41 (d, J = 7.6 Hz, 1H, $C^4H_{(Ar)}$), 5.33 (s, 1H, $CH(OMe)_2$), 4.07 (d, J = 13.9 Hz, 1H, C^7H_2), 3.82 (d, J = 13.8 Hz, 1H, C^7H_2), 3.66 (s, 3H, CH_3), 3.54–3.30 (7H, $C^8H_{(Pro)}$, $(OCH_3)_2$), 3.14–3.04 (m, 1H, $C^{11}H_{2(Pro)}$), 2.54 (dd, J = 16.8, 8.1 Hz, 1H, $C^{11}H_{2(Pro)}$), 2.21–2.09 (m, 1H, $C^9H_{2(Pro)}$), 2.02–1.75 (m, 3H, $C^9H_{2(Pro)}$, $C^{10}H_{2(Pro)}$).

(*R*)-methyl-1-(dimethoxymethyl)pyridine-2-yl-methyl-pyrrolidine-2-carboxylate. A solution of D-proline methylester hydrochloride (1.23 g, 7.44 mmol) in CH_2Cl_2 (11 mL) was treated with triethylamine (2.06 mL, 14.9 mmol) in THF (6 mL) and then combined with a solution of protected aldehyde (1.00 g, 4.96 mmol) in THF (11 mL). Then the reaction mixture was heated at 40 °C overnight. The white precipitate of triethylammonium chloride was filtered off to give a slightly yellow clear solution, which was freed from solvent under reduced pressure and the oily residue was purified by column chromatography using a mixture of $CHCl_3$:MeOH 97.5:2.5 as eluent. The product was obtained after removal of the solvent as a slightly yellow oil. Yield: 0.89 g, 61%. ^{1}H NMR (500 MHz, $CDCl_3$): δ 7.69 (t, J = 7.7 Hz, 1H, $C^5H_{(Ar)}$), 7.46 (d, J = 7.0 Hz, 1H, $C^6H_{(Ar)}$), 7.41 (d, J = 7.6 Hz, 1H, $C^4H_{(Ar)}$), 5.33 (s, 1H, $CH(OMe)_2$), 4.07 (d, J = 13.9 Hz, 1H, C^7H_2), 3.82 (d, J = 13.8 Hz, 1H, C^7H_2), 3.66 (s, 3H, CH_3), 3.54–3.30 (7H, $C^8H_{(Pro)}$, $(OCH_3)_2$), 3.14–3.04 (m, 1H, $C^{11}H_{2(Pro)}$), 2.54 (dd, J = 16.8, 8.1 Hz, 1H, $C^{11}H_{2(Pro)}$), 2.21–2.09 (m, 1H, $C^9H_{2(Pro)}$), 2.02–1.75 (m, 3H, $C^9H_{2(Pro)}$, $C^{10}H_{2(Pro)}$).

(*S*)-1-((6-formylpyridin-2-yl)methyl)pyrrolidine-2-carboxylic acid. (*S*)-methyl-1-((dimethoxymethyl)pyridine-2-yl)methyl)pyrrolidine-2-carboxylate (0.63 g, 2.1 mmol) in water (12 mL)

was heated at reflux for 48 h. The solvent was removed under reduced pressure yielding red, highly viscous oil, which gave a red solid after drying in vacuo. Yield: 0.50 g, 100%. ^{1}H NMR (500 MHz, DMSO-d_6): δ 9.96 (s, 1H, C*H*O), 8.03 (dd, J = 7.7, 7.2 Hz, 1H, $C^5H_{(Ar)}$), 7.87–7.75 (m, 2H, $C^6H_{(Ar)}$), $C^4H_{(Ar)}$), 4.19 (d, J = 14.3 Hz, 1H. C^7H_2), 3.90 (d, J = 14.3 Hz, 1H, C^7H_2), 3.42 (dd, J = 8.9, 5.6 Hz, 1H, $C^8H_{(Pro)}$, overlapped water peak), 3.02 (ddd, J = 9.0, 7.4, 3.9 Hz, 1H, $C^{11}H_{2(Pro)}$), 2.58–2.52 (m, 1H, $C^{11}H_{2(Pro)}$, overlapped solvent peak), 2.18–2.07 (m, 1H, $C^9H_{2(Pro)}$), 1.91–1.67 (m, 3H, $C^9H_{2(Pro)}$, $C^{10}H_{2(Pro)}$).

(*R*)-1-((6-formylpyridin-2-yl)methyl)pyrrolidine-2-carboxylic acid. (*R*)-methyl-1-((dimethoxymethyl)pyridine-2-yl)methyl)pyrrolidine-2-carboxylate (0.89 g, 3.02 mmol) in water (20 mL) was heated at reflux for 48 h. The solvent was removed under reduced pressure yielding a red, highly viscous oil which gave a red solid after drying in vacuo. Yield: 0.71 mg, 100%. ^{1}H NMR (500 MHz, DMSO-d_6): δ 9.96 (s, 1H, C*H*O), 8.03 (dd, J = 7.7, 7.2 Hz, 1H, $C^5H_{(Ar)}$), 7.87–7.75 (m, 2H, $C^6H_{(Ar)}$), $C^4H_{(Ar)}$), 4.19 (d, J = 14.3 Hz, 1H. C^7H_2), 3.90 (d, J = 14.3 Hz, 1H, C^7H_2), 3.42 (dd, J = 8.9, 5.6 Hz, 1H, $C^8H_{(Pro)}$, overlapped water peak), 3.02 (ddd, J = 9.0, 7.4, 3.9 Hz, 1H, $C^{11}H_{2(Pro)}$), 2.58–2.52 (m, 1H, $C^{11}H_{2(Pro)}$, overlapped solvent peak), 2.18–2.07 (m, 1H, $C^9H_{2(Pro)}$), 1.91–1.67 (m, 3H, $C^9H_{2(Pro)}$, $C^{10}H_{2(Pro)}$).

L-Pro-FTSC. (*S*)-1-((6-formylpyridin-2-yl)methyl)pyrrolidine-2-carboxylic acid (0.30 g, 1.27 mmol) and thiosemicarbazide (0.12 g, 1.27 mmol) in a 25 mL Schlenk-tube were suspended in ethanol (5 mL). The mixture was heated at 78 °C for 24 h. After cooling down the white precipitate was filtered off under argon atmosphere, washed with ethanol (2.5 mL) and diethyl ether (2 × 2 mL) and dried in vacuo. Yield: 0.26 g, 67%. Anal. Calcd for $C_{13}H_{17}N_5O_2S{\cdot}0.9H_2O$ (M_r 323.95 g/mol), %: C, 48.25; H, 5.86; N, 21.64; S, 9.91. Found, %: C, 48.58; H, 5.86; N, 21.20; S, 9.88. ^{1}H NMR (500 MHz, DMSO-d_6): δ 11.66 (s, 1H, H^2), 8.33 (s, 1H, H^3), 8.18–8.14 (m, 2H, H^6, H^3) 8.05 (s, 1H, H^{13}), 7.82 (t, J = 7.8 Hz, 1H, H^5), 7.45 (d, J = 7.5 Hz, 1H, H^4), 4.13 (d, J = 14.1 Hz, 1H, H^7), 3.86 (d, J = 14.0 Hz, 1H, H^7), 3.44 (dd, J = 8.9, 5.4 Hz, 1H, H^8), 3.07 (ddd, J = 9.4, 7.6, 3.6 Hz, 1H, H^{11}), 2.62–2.55 (m, 1H, H^{11}), 2.15–2.07 (m, 1H, H^9), 1.92–1.85 (m, 1H, H^9), 1.84–1.66 (m, 2H, H^{10}). ^{13}C NMR (126 MHz, DMSO) δ 178.87 (Cq, C^{14}), 173.79 (Cq, C^{12}), 157.62 (Cq, C^3), 153.16 (Cq, C^1), 142.74 (CH, C^{13}), 137.59 (CH, C^5), 123.77 (CH, C^4), 119.46 (CH, C^6), 66.19 (CH, C^8), (59.24 (CH_2, C^7), 53.55 (CH_2, C^{11}), 29.25 (CH_2, C^9),

23.66, (CH_2, C^{10}). Solubility in water: ≥ 1.56 mol/L. ESI-MS (methanol), positive: *m/z* 308 $[M+H]^+$. IR (ATR, selected bands, ν_{max}): 3425, 2972, 1623, 1586, 1529, 1438, 1385, 1275 1109, 829, 638 cm^{-1}.

D-Pro-FTSC. (*R*)-1-((6-formylpyridin-2-yl)methyl)pyrrolidine-2-carboxylic acid (0.30 g, 1.27 mmol) and thiosemicarbazide (0.12 g, 1.27 mmol) in a 25 mL Schlenk-tube were suspended in ethanol (5 mL). The mixture was heated at 78 °C for 24 h. After cooling down the white precipitate was filtered off under argon atmosphere, washed with ethanol (2.5 mL) and diethyl ether (2 × 2 mL) and dried in vacuo. Yield: 227 mg, 58%. Anal. Calcd for $C_{13}H_{17}N_5O_2S{\cdot}0.7H_2O$ (M_r 319.98 g/mol): C, 48.80; H, 5.80; N, 21.88; S, 10.02. Found, %: C, 48.96; H, 5.77; N, 21.50; S, 9.70. ^{1}H NMR (500 MHz, DMSO-d_6): δ 11.66 (s, 1H, H^2), 8.33 (s, 1H, H^3), 8.18–8.14 (m, 2H, H^6, H^3) 8.05 (s, 1H, H^{13}), 7.82 (t, *J* = 7.8 Hz, 1H, H^5), 7.45 (d, *J* = 7.5 Hz, 1H, H^4), 4.13 (d, *J* = 14.1 Hz, 1H, H^7), 3.86 (d, *J* = 14.0 Hz, 1H, H^7), 3.44 (dd, *J* = 8.9, 5.4 Hz, 1H, H^8), 3.07 (ddd, *J* = 9.4, 7.6, 3.6 Hz, 1H, H^{11}), 2.62−2.55 (m, 1H, H^{11}), 2.15−2.07 (m, 1H, H^9), 1.92−1.85 (m, 1H, H^9), 1.84−1.66 (m, 2H, H^{10}). ^{13}C NMR (126 MHz, DMSO) δ 178.87 (Cq, C^{14}), 173.79 (Cq, C^{12}), 157.62 (Cq, C^3), 153.16 (Cq, C^1), 142.74 (CH, C^{13}), 137.59 (CH, C^5), 123.77 (CH, C^4), 119.46 (CH, C^6), 66.19 (CH, C^8), (59.24 (CH_2, C^7), 53.55 (CH_2, C^{11}), 29.25 (CH_2, C^9), 23.66, (CH_2, C^{10}). Solubility in water: ≥ 1.56 mol/L. ESI-MS (methanol), positive: *m/z* 308 $[M+H]^+$. IR (ATR, selected bands, ν_{max}): 3425, 2972, 1623, 1586, 1529, 1438, 1385, 1275 1109, 829, 638 cm^{-1}.

Synthesis of copper(II) complexes

[Cu(L-Pro-FTSC)]·0.9H$_2$O or [Cu(*S*,*R*-L)]·0.9H$_2$O. To a solution of L-Pro-FTSC (0.12 g, 0.39 mmol) in water (20 mL) was added a solution of copper(II) acetate monohydrate (0.16 g, 0,78 mmol) in water (5 mL). The color of the solution changed from colorless to dark green and the solution was heated at 70 °C for 1 h. After cooling down the reaction mixture was concentrated under reduced pressure to about 5 mL and allowed to stand at 4 °C. The green crystals were filtered off, washed with water and dried in vacuo. Yield: 101 mg, 70%. Anal. Calcd for $C_{13}H_{15}CuN_5O_2S{\cdot}0.9H_2O$ (M_r 385.12 g/mol), %: C, 40.54; H, 4.40; N, 18.19; S, 8.33. Found, %: C, 40.78; H, 4.63; N, 17.97; S, 8.32. Solubility in water: ≥ 4.15 mmol/L; DMSO: ≥ 11.53 mmol/L. ESI-MS (methanol), positive: *m/z* 369 $[M+H]^+$. IR (ATR, selected bands, ν_{max}): 3442, 3278, 3164, 1584, 1457, 1378, 1311, 1159, 642, 603 cm^{-1}.

[Cu(D-Pro-FTSC)]·H_2O or [Cu(*R*,*S*-L)]·H_2O. To D-Pro-FTSC (0.10 g, 0.32 mmol) in water (20 mL) was added copper(II) acetate monohydrate (0.13 mg, 0.65 mmol) in water (5 mL). The color of the solution changed from colorless to dark green and the solution was heated at 70 °C and stirred for 1 h. After cooling down the reaction mixture was concentrated under reduced pressure to a volume of about 5 mL and left in the fridge overnight. The next day green crystals were filtered off, washed with water and dried under reduced pressure. Yield: 65 mg, 55%. Anal. Calcd for $C_{13}H_{15}CuN_5O_2S·H_2O$ (M_r 386.92 g/mol), %: C, 40.35; H, 4.43; N, 18.10; S, 8.29. Found, %: C, 40.66; H, 4.05; N, 17.72; S, 8.34. Solubility in water: ≥ 4.15 mmol/L; DMSO: ≥ 11.53 mmol/L. ESI-MS (methanol), positive: *m/z* 369 $[M+H]^+$. IR (ATR, selected bands, ν_{max}): 3442, 3278, 3164, 1584, 1457, 1378, 1311, 1159, 642, 603 cm^{-1}.

pH-potentiometric measurements

The purity and aqueous phase stability of the ligand L-Pro-FTSC was verified and the exact concentrations of the stock solutions prepared were determined by the Gran method.[50] The pH-metric measurements for determination of the protonation constants of the ligand and the overall stability constants of the copper(II) complexes were carried out at 298.0 ± 0.1 K in water and at an ionic strength of 0.10 M (KCl, Sigma-Aldrich) in order to keep the activity coefficients constant. Since in the previous studies on various TSCs 30% (w/w) DMSO/H_2O solvent mixture was always used,[32–] in order to obtain comparable data the same conditions were also applied. The titrations were performed with carbonate-free KOH solution of known concentration (0.10 M). Both the base and the HCl were Sigma-Aldrich products and their concentrations were determined by pH-potentiometric titrations. An Orion 710A pH-meter equipped with a Metrohm combined electrode (type 6.0234.100) and a Metrohm 665 Dosimat burette were used for the pH-metric measurements. The electrode system was calibrated to the pH = $\log[H^+]$ scale in water and in the DMSO/water solvent mixture by means of blank titrations (strong acid vs strong base; HCl vs KOH), according to the method suggested by Irving *et al.*[51] The average water ionization constant, pK_w, is 13.76 ± 0.01 with pure water and 14.52 ± 0.05 with DMSO/water 30:70 (w/w) as solvent at 25 °C, which corresponds well to the literature data.[52] The reproducibility of the titration points included in the calculations was within 0.005 pH. The pH-metric titrations were

performed in the pH range 2.0 – 11.5 (or 12.5 in the 30% (w/w) DMSO/water mixture). The initial volume of the samples was 5.0 mL. The ligand concentration was in the range $1.6 - 1.8 \times 10^{-3}$ M and metal ion-to-ligand ratios of 1:1 – 1:4 were used. The accepted fitting of the titration curves was always less than 0.01 mL. Samples were deoxygenated by bubbling purified argon through them for *ca.* 10 min prior to the measurements.

The protonation constants of the ligands were determined with the computer program SUPERQUAD.[53] PSEQUAD[54] was utilized to establish the stoichiometry of the complexes and to calculate the stability constants ($\log\beta(M_pL_qH_r)$). $\beta(M_pL_qH_r)$ is defined for the general equilibrium $pM + qL + rH \rightleftharpoons M_pL_qH_r$ as $\beta(M_pL_qH_r) = [M_pL_qH_r]/[M]^p[L]^q[H]^r$, where M denotes the metal ion and L the completely deprotonated ligand. In all calculations exclusively titration data were used from experiments, in which no precipitate was visible in the reaction mixture.

UV–vis spectrophotometric, spectrofluorimetric, CD and ^{1}H NMR measurements. A Hewlett Packard 8452A diode array spectrophotometer was used to record the UV–vis spectra in the 200 to 820 nm window. The path length was 1 or 2 cm. Protonation and stability constants and the individual spectra of the species were calculated by the computer program PSEQUAD.[54] The spectrophotometric titrations were performed on samples of the L-Pro-FTSC alone or with copper(II) ions; the concentration of the ligand was 4.2×10^{-5} M (L-Pro-FTSC alone) or 2×10^{-3} M (for copper(II) containing samples) and the metal-to-ligand ratios were 0:1, 1:1 and 1:2 over the pH range between 2 and 11.5 at an ionic strength of 0.10 M (KCl) in water at 298.0 ± 0.1 K. Measurements for the ligand alone and copper(II) – L-Pro-FTSC systems at metal-to-ligand ratio 1:1 were also carried out by preparing individual samples, in which the 0.1 M KCl was partially or completely replaced by HCl and pH values, varying in the range *ca.* 1.0 – 1.8, were calculated from the HCl content. For the calculation of the stability constants of the protonated mono-ligand copper(II) – L-Pro-FTSC complexes mainly CT bands (which are strongly overlapped with the ligand bands) were used (λ = 220 – 440 nm).

UV–vis spectrophotometric measurements on systems containing HSA at $0 - 2 \times 10^{-4}$ M and 2.2×10^{-5} M L-Pro-FTSC, 2.2×10^{-5} M copper(II) and 4-(2-hydroxyethyl)-1-piperazineethanesulfonic acid (HEPES) at 0.02 M as buffer at pH 7.40 were performed in order to obtain the difference spectra.

Control measurements were carried out under the same conditions with samples containing only HSA at various concentrations and HEPES buffer.

The pH-dependent fluorescence measurements were carried out on a Hitachi-4500 spectrofluorometer with the excitation at 320 nm. The emission spectra were recorded using 10 nm/10 nm slit widths in 1 cm quartz cell in the pH range between 2 and 11.5 at 298.0 ± 0.1 K. Samples contained 1.0×10^{-5} M L-Pro-FTSC ligand at 0.1 M (KCl) ionic strength. Three-dimensional spectra were recorded at 230 – 500 nm excitations and at 240 – 600 nm emission wavelengths for the 1.0×10^{-5} M ligand containing samples at pH 7.0 using 10 nm/10 nm slit widths.

One dimensional ^{1}H and ^{13}C NMR and two dimensional ^{1}H-^{1}H COSY, ^{1}H-^{1}H TOCSY, ^{1}H-^{1}H TOCSY, ^{1}H-^{1}H ROESY or ^{1}H-^{1}H NOESY, ^{1}H-^{13}C HSQC and ^{1}H-^{13}C HMBC NMR spectra were recorded on two Bruker Avance III instruments. DMSO-d_6 or $CDCl_3$ were used as solvent. ^{1}H or ^{13}C chemical shifts were measured relatively to the solvent peaks.

The pH-dependent ^{1}H NMR studies were carried out on a Bruker Ultrashield 500 Plus instrument. 4,4-Dimethyl-4-silapentane-1-sulfonic acid was used as an internal NMR standard. L-Pro-FTSC was dissolved in a 10% (v/v) D_2O /H_2O mixture in a concentration of 1.0×10^{-3} M. The direct pH-meter readings were corrected according to method of Irving *et al.*[51] Binding of the ligand L-Pro-FTSC to HSA was measured by ^{1}H NMR spectroscopy at pH 7.40 in the aqueous solution of the HEPES buffer (0.02 M). Samples contained 8.3×10^{-4} M *L*-Pro-FTSC and 4.2×10^{-4} M HSA in the presence of 10% (v/v) D_2O. Samples were incubated for 24 h at 298 K.

CD spectra were recorded on a Jasco J-815 spectrometer in an optical cell of 1 or 2 cm path length. The analytical concentration of the copper(II) − D- or L-Pro-FTSC complexes was 4.0×10^{-5} M at pH 7.4 in aqueous solution and spectra were recorded in the wavelength interval from 250 to 450 nm. 2.0×10^{-3} M ligand concentration was used for the copper(II) − L-Pro-FTSC system at 1:1 metal-to-ligand ratio. pH was varied between 2 and 11.5 and spectra were analyzed in the range of 525 − 800 nm. CD data are given as the differences in molar absorptivities between left and right circularly polarized light, based on the concentration of the ligand ($\Delta\varepsilon = \Delta A / l / c_{\text{ligand or complex}}$).

Determination of the distribution coefficient (*D*). *D* values of L- and D-Pro-FTSC and their copper(II) complexes were determined by the traditional shake-flask method in *n*-octanol/buffered aqueous solution at pH 7.4 (HEPES buffer) at 298.0 ± 0.2K as described previously.[32,33] Two parallel experiments were performed for each sample. The ligands were dissolved at 1.0×10^{-4} M and the complexes in 1.0×10^{-4} M in the *n*-octanol pre-saturated aqueous solution of the buffer (0.02 M) at constant ionic strength (0.10 M KCl). The aqueous solutions and *n*-octanol with 1:1 phase ratio were gently mixed with 360° vertical rotation for 3 h to avoid the emulsion formation, and the mixtures were centrifuged at 5000 rpm for 3 min by a temperature controlled centrifuge (Sanyo) at 298K. After separation UV−vis spectra of the ligands or complexes in the aqueous phase were compared to those of the original aqueous solutions. As no measurable amount of the ligands or the copper(II) complexes was found in the *n*-octanol phase, $D_{7.4}$ values were merely estimated.

EPR measurements and deconvolution of the spectra. X-band-EPR spectra were recorded with a BRUKER EleXsys E500 spectrometer (microwave frequency 9.81 GHz, microwave power 10 mW, modulation amplitude 5 G, modulation frequency 100 kHz). During titration, the isotropic EPR spectra were recorded at room temperature in a circulating system. EPR spectra were recorded for samples with 1:1 copper(II)-to-ligand ratios, respectively at 1.0×10^{-3} M L-Pro-FTSC concentration between pH 1.7 and 11.8 in water at $I = 0.10$ M (KCl). KOH solution was added to the stock solution to adjust the pH which was measured with a Radiometer PHM240 pH/ion Meter equipped with a Metrohm 6.0234.100 glass electrode. A Heidolph Pumpdrive 5101 peristaltic pump was used to circulate the solution from the titration pot through a capillary tube into the cavity of the instrument. The titrations were carried out under nitrogen atmosphere. 0.1 mL of sample was taken out of the stock solution at various pH values and was measured individually in a dewar containing liquid nitrogen (at 77 K) under the same instrumental conditions as the room-temperature spectra described above. 0.02 mL of methanol was added to the samples to avoid water crystallization. Interaction of complex [CuL] with proteins and amino acids (HSA/MEM) was tested two hours after preparation, under the same instrumental conditions as above, at room temperature. The EPR spectra were recorded for samples contained (1) 1.0 mM complex dissolved in HEPES buffer (pH = 7.4, $I = 0.1$ M KCl), (2) 1 mM complex and 0.5 mM HSA dissolved in HEPES, and (3) 1 mM complex in MEM.

Series of pH-dependent room-temperature CW-EPR spectra were simulated simultaneously by the „two-dimensional" method using the 2D_EPR program.[55] Each component curve was described by the isotropic EPR parameters g_o, A_o^{Cu} copper hyperfine and A_o^N nitrogen hyperfine couplings, and the relaxation parameters α, β, γ which define the line widths in the equation $\sigma_{MI} = \alpha + \beta M_I + \gamma M_I^2$, where M_I denotes the magnetic quantum number of copper nucleus. The concentrations of the complexes were varied by fitting their formation constants $\beta(M_pL_qH_r)$ defined by the general equilibrium found in the pH-potentiometric studies section.

The anisotropic spectra recorded at 77 K were analyzed individually with the EPR program,[56] which gives the anisotropic EPR parameters g_x, g_y, g_z (rhombic g-tensor), A_x^{Cu}, A_y^{Cu}, A_z^{Cu} (rhombic copper hyperfine tensor) and A_x^N, A_y^N, A_z^N (rhombic nitrogen superhyperfine tensor) and the orientation dependent line width parameters. All tensors were supposed as coaxial.

The EPR spectra of the dimeric complex was simulated by a new modul of the 'EPR' program[51] developed for calculating EPR spectra and dynamic nuclear polarization (DNP) in coupled spin systems (biradicals and paramagnetic dimers). The EPR spectrum is calculated by the complete diagonalization of the Hamiltonian of a two-spin system:

$$H_{SH} = \vec{H} * \hat{g}_1 * \vec{S}_1 . \mu_B + \vec{H} * \hat{g}_2 * \vec{S}_2 . \mu_B + J\vec{S}_1\vec{S}_2 + D\left(2S_{z1}S_{z2} - S_{x1}S_{x2} - S_{y1}S_{y2}\right) + \vec{S}_1 * \hat{A}_1 * \vec{I}_1 + \vec{S}_2 * \hat{A}_2 * \vec{I}_2$$

where g_1, A_1 and g_2, A_2 are the g-, and A-tensors of the copper(II) centres, D is the dipolar interaction and J is the exchange interaction between the two spin centres. The principal values and principal orientation of g- and A-tensors can be treated identically or differently and their relative orientation can be characterized by the three Euler angles (α,β and γ). The relative position of the two centres is further described by two polar angle (χ,ψ) which define the position of the connector line between the copper(II) centres in the frame of g_1.

Since a natural $CuCl_2$ was used for the measurements, the spectra were calculated as the sum of the spectra of ^{63}Cu and ^{65}Cu weighted by their natural abundances. The quality of fit was characterized by the noise-corrected regression parameter R_j as above. The details of the statistical analysis were

published previously.[55] The copper and nitrogen coupling constants and the relaxation parameters were obtained in field units (Gauss = 10^{-4} T)

Crystallographic Structure Determination. X-ray diffraction measurements were performed on a Nonius Kappa CCD diffractometer. Single crystal was positioned at 35 mm from the detector, and 644 frames were measured, each for 25 s over 1.5° scan width. The data were processed using DENZO software.[57] Crystal data, data collection parameters, and structure refinement details are given in Table 4. The structure was solved by direct methods and refined by full-matrix least-squares techniques. Non-H atoms were refined with anisotropic displacement parameters. H atoms were inserted in calculated positions and refined with a riding model. The following computer programs and hardware were used: structure solution, *SHELXS-97* and refinement, *SHELXL-97*;[58] molecular diagrams, ORTEP;[59] computer, Intel CoreDuo.

Table 4. Crystal Data and Details of Data Collection for [Cu(R_N,S_C)-L)]·2H_2O.

compound	[Cu(R_N,S_C)-L]·2H_2O
empirical formula	$C_{13}H_{19}CuN_5O_4S$
fw	404.93
space group	$P2_12_12_1$
a, Å	7.4900(1)
b, Å	10.0006(1)
c, Å	21.5284(3)
V [Å^3]	1612.57(4)
Z	4
λ [Å]	0.71073
ρ_{calcd}, g cm^{-3}	1.668
cryst size, mm^3	0.30 × 0.30 × 0.10
T [K]	110(2)
μ, mm^{-1}	1.513
R_1[a]	0.0271
wR_2[b]	0.687
Flack parameter	−0.012(8)
GOF[c]	1.032

[a] $R_1 = \Sigma||F_o| - |F_c||/\Sigma|F_o|$. [b] $wR_2 = \{\Sigma[w(F_o^2 - F_c^2)^2]/\Sigma[w(F_o^2)^2]\}^{1/2}$. [c] GOF = $\{\Sigma[w(F_o^2 - F_c^2)^2]/(n - p)\}^{1/2}$, where n is the number of reflections and p is the total number of parameters refined.

Cell lines and culture conditions. Human CH1 (ovarian carcinoma) and SW480 (colon carcinoma) cell lines were kindly provided by Lloyd R. Kelland (CRC Centre for Cancer Therapeutics, Institute of Cancer Research, Sutton, UK) and Brigitte Marian (Institute of Cancer Research, Medical University of Vienna, Austria), respectively. The cells were cultured in MEM supplemented with 10% heat-inactivated fetal bovine serum, 1 mM sodium pyruvate, 4 mM glutamine and 1% (v/v) nonessential amino acids (from 100-times ready-to-use stock solution), all purchased from Sigma-Aldrich, and maintained at 37 °C in a humidified atmosphere containing 5% CO_2.

Cytotoxicity Tests in Cancer Cell lines. Cytotoxic effects of the test compounds were determined by means of a colorimetric microculture assay [MTT assay, MTT = 3-(4,5-dimethyl-2-thiazolyl)-2,5-diphenyl-2H-tetrazolium bromide]. Cells grown as adherent monolayer in 75 cm^3 flasks (CytoOne/ Starlabs, Germany) were harvested by trypsinisation. By using a pipetting robot (Biotek Precision XS Microplate Sample Processor), densities of 1×10^3 (CH1) and 2×10^3 (SW480) were seeded, as triplicates, in 100 µl aliquots in 96-well microculture plates (CytoOne/ Starlabs, Germany). Before the drug exposure, cells were allowed to settle and attach in drug-free complete culture medium for 24 h. Test compounds were dissolved in distilled water prior to the preparation of a serial dilution in complete culture medium. The dilution series as well as the pipetting steps were done by the microplate processor. After 96 h of exposure, the medium was removed and replaced by 100 µl 1:7 MTT/RPMI 1640 solution (MTT solution: 5 mg/ml MTT in phosphate buffered saline; RPMI: supplemented with 10% heat-inactivated fetal bovine serum and 4 mM glutamine) and incubated for 4 h at 37 °C in a humidified atmosphere with 5% CO_2. Subsequently the MTT/RPMI solution was removed from all wells and the formazan crystals formed by viable cells were dissolved in 150 µl DMSO per well. Optical densities at 550 nm were measured with a microplate reader (Biotek ELx808), using a reference wavelength of 690 nm to correct for unspecific absorption. The quantity of viable cells was expressed in terms of the T/C values by a comparison to untreated control microcultures, and 50% inhibitory concentrations (IC_{50}) were calculated from concentration-effect curves by interpolation. Evaluation is based on means from at least three independent experiments.

Topoisomerase IIα inhibition. The Topo IIα inhibition capacity of the L- and D-Pro-FTSC compounds and their corresponding copper(II) complexes was determined by means of the DNA plasmid relaxation

assay. For this purpose we used the topoisomerase drug screening kit and the human recombinant Topo IIα enzyme from TopoGen Inc. The supercoiled pHOT1 plasmid DNA was used as a substrate and was incubated for 30 min at 37° C with Topo IIα in the presence of various concentrations of the Pro-FTSC compounds. As positive control Etoposide (2 mM) was used. The reaction was stopped by rapid addition of 10% SDS followed by digestion with proteinase K. The products of the reaction were separated on a 1% agarose gel and analysed by visualization with ethidium bromide (0.5 μg/ml) via the detection system Fusion SL (Vilber Lourmat). Evaluation is based on two independent experiments.

Supporting Information Available: Portion of the crystal structure showing intermolecular hydrogen bonding interactions (Figure S1), UV–vis molar absorbance and CD spectra of the copper(II) complexes (Figure S2), pH dependence of the chemical shifts of the various protons of the ligand L-Pro-FTSC with its concentration distribution curve (Figure S3), 3D fluorescence spectrum of L-Pro-FTSC at pH 7.0 in water (A) and its pH-dependent fluorescence spectra at 320 nm excitation (B) (Figure S4), UV–vis absorbance spectra of copper(II) – L-Pro-FTSC complex at different pH values (A) and concentration distribution curves for the relevant system with the pH-dependent absorbance at 610 nm (B) (Figure S5), CD spectra of copper(II) – L-Pro-FTSC complex at different pH (Figure S6), EPR spectra of copper(II) – L-Pro-FTSC complex at pH 5.3 (Figure S7), experimental and calculated EPR spectra of copper(II) – HSA (A), [CuL] in HEPES buffer (B), in the presence of HSA (C) and in MEM (D) (Figure S8), UV–vis absorbance spectra of copper(II) – L-Pro-FTSC – HSA at pH 7.40 at different HSA concentrations (Figure S9). This material is available free of charge via the Internet at http://pubs.acs.org.

Author Information

Corresponding Author

* E-mail: enyedy@chem.u-szeged.hu (E.A.E.); vladimir.arion@univie.ac.at (V.B.A.).

Acknowledgments. We thank Prof. Gerald Giester for collection of X-ray data, Dr. M. A. Jakupec for discussion of biological part of the work and Mag. A. A. Dobrov for ESI mass spectrometry measurements.

References

(1) Casas, J. S.; Garcia-Tasende, M. S.; Sordo, J. *Coord. Chem. Rev.* **2000**, *209*, 197–261.

(2) West, D. X.; Padhye, S. B.; Sonawane, P. B. *Struct. Bond.* **1991**, *76*, 1–50.

(3) Garcia-Tojal, J.; Gil-Garcia, R.; Gomez-Saiz, P.; Ugalde, M. *Curr. Inorg. Chem.* **2011**, *1*, 189–210.

(4) Mahajan, R. K.; Walia, T. P. S.; Sumanjit, L. T. S. *Talanta* **2005**, *67*, 755–759.

(5) Beraldo, H.; Gambino, D. *Mini-Rev. Med. Chem.* **2004**, *4*, 31–39.

(6) Brockman, R. W.; Thomson, J. R.; Bell, M. J.; Skipper, H. E. *Cancer Res.* **1956**, *16*, 167–170.

(7) Wadler, S.; Makower, D.; Clairmont, C.; Lambert, K.; Fehn, K.; Sznol, M.; *J. Clin. Oncol.* **2004**, *22*, 1553–1563.

(8) Mackenzie, M. J.; Saltman, D.; Hirte, H.; Low, J.; Johnson, C.; Pond, G.; Moore, M. J. *Invest. New Drugs* **2007**, *25*, 553–558.

(9) Kolesar, J.; Brundage, R. C.; Pomplun, M.; Alberti, D., Holen, K.; Traynor, A.; Ivy, P.; Wilding, G. *Cancer Chemother. Parmacol.* **2011**, *67*, 393–400.

(10) Attia, S.; Kolesar, J.; Mahoney, M. R.; Pitot, H. C.; Laheru, D.; Heun, J.; Huang, W.; Eickhoff, J.; Erlichman, C.; Holen, K. D. *Invest. New Drugs* **2008**, *26*, 369–379.

(11) Karp, J. E., Giles, F. J.; Gojo, I.; Morris, L.; Greer, J.; Johnson, B.; Thein, M.; Sznol, M.; Low, J. *Leuk. Res.* **2008**, *32*, 71–77.

(12) Kolberg, M.; Strand, K. R.; Graff, P.; Andersson, K. K. *Biochim. Biophys. Acta* **2004**, *1699*, 1–34.

(13) Moore, E. C.; Zedeck, M. S.; Agrawal, K. C.; Sartorelli, A. C. *Biochemistry* **1970**, *9*, 4492–4498.

(14) French, F. A.; Blanz, E. J.; Shaddix, S. C.; Brockman, R. W. *J. Med. Chem.* **1974**, *17*, 172–181.

(15) Kowol, C. R.; Berger, R.; Eichinger, R.; Roller, A.; Jakupec, M. A.; Schmidt, P. P.; Arion, V. B.; Keppler, B. K. *J. Med. Chem.* **2007**, *50*, 1254–1265.

(16) Kalinowski, D. S.; Richardson, D. R. *Pharmacol. Rev.* **2005**, *57*, 547–583.

(17) Chaston, T. B.; Lovejoy, D. B.; Watts, R. N.; Richardson, D. R. *Clin. Cancer Res.* **2003**, 402–414.

(18) Cooper, C. E.; Lynagh, G. R.; Hoyes, K. P.; Hider, R. C.; Cammack, R.; Porter, J. B. *J. Biol. Chem.* **1996**, *271*, 20291–20299.

(19) Shao, J.; Zhou, B.; Di Bilio, A. J.; Zhu, L.; Wang, T.; Qi, C.; Shih, J.; Yen, Y. *Mol. Canc. Ther.* **2006**, *5*, 586–592.

(20) Thelander, L.; Gräslund, A. *J. Biol. Chem.* **1982**, *258*, 4063–4066.

(21) Aye, Y.; Long, M. J. C.; Stubbe, J. *J. Biol. Chem.* **2012**, *287*, 35768–35778.

(22) Nitiss, J. L. *Nature Rev. Cancer* **2009**, *9*, 327–337.

(23) Schoeffler, A. J.; Berger, J. M. *Q. Rev. Biophys.* **2008**, *41*, 41–101.

(24) Easmon, J.; Puerstinger, G.; Heinisch, G.; Roth, T.; Fiebig, H. H.; Holzer, W.; Jaeger, W.; Jenny, M.; Hofmann, J. *J. Med. Chem.* **2001**, *44*, 2164–2171.

(25) Wei, L.; Easmon, J.; Nagi, R. K.; Muegge, B. D.; Meyer, L. A.; Lewis, J. S. *J. Nucl. Med.* **2006**, *47*, 2034–2041.

(26) Huang, H.; Chen, Q.; Ku, X.; Meng, L.; Wang, X.; Zhu, C.; Wang, Y.; Chen, Z.; Li, M.; Jiang, H.; Chen, K.; Ding, J.; Liu, H. *J. Med. Chem.* **2010**, *53*, 3048–3064.

(27) Zeglis, B. M.; Divilov, V.; Lewis, J. S. *J. Med. Chem.* **2011**, *54*, 2391–2398.

(28) Bailly, C. *Chem. Rev.* **2012**, *112*, 3611–3640.

(29) Rao, V. A.; Klein, S. R.; Agama, K. K.; Toyoda, E.; Adachi, N.; Pommier, Y.; Shacter, E. B. *Cancer Res.* **2009**, *69*, 948–957.

(30) (a) Richardson, D. R.; Sharpe, P. C.; Lovejoy, D. B.; Senaratne, D.; Kalinowski, D. S.; Islam, M.; Bernhardt, P. V. *J. Med. Chem.* **2006**, *49*, 6510–6521; (b) Opletalova, V.; Kalinowski, D. S.; Vejsova, M.; Kunes, J.; Pour, M.; Jampilek, J.; Buchta, V.; Richardson, D. R. *Chem. Res. Toxicol.* **2008**, *21*, 1878–1889; (c) Jansson, P. J.; Sharpe, P. C.; Bernhardt, P. V.; Richardson, D. R. *J. Med. Chem.* **2010**, *53*, 5759–5769; (d) Kalinowski, D. S.; Yu, Y.; Sharpe, P. C.; Bernhardt, P. V.; Richardson, D. R. *J. Med. Chem.* **2007**, *50*, 3716–3729; (e) Richardson, D. R.; Kalinowski, D. S.; Richardson, V.; Sharpe, P. C.; Lovejoy, D. B.; Islam, M.; Bernhardt, P. J. *J. Med. Chem.* **2009**, *52*, 1459–1470.

(31) Knight, J. M.; Whelan, H.; Petering, D. H. *J. Inorg. Biochem.* **1979**, *11*, 327–338

(32) Milunovic, M. N. M.; Enyedy, E. A.; Nagy, N. V.; Kiss, T.; Trondl, R.; Jakupec, M. A.; Keppler, B. K.; Krachler, R.; Novitchi, G.; Arion, V. B. *Inorg. Chem.* **2012**, *51*, 9309–9321.

(33) Enyedy, É. A.; Zsigó, É.; Nagy, N. V.; Kowol, C. R.; Roller, A.; Keppler, B. K.; Kiss, T.; *Eur. J. Inorg. Chem.* **2012**, 4036–4047.

(34) Enyedy, É. A.; Primik, M. F.; Kowol, C. R.; Arion, V. B.; Kiss, T.; Keppler, B. K. *Dalton Trans.* **2011**, *40*, 5895–5905.

(35) Enyedy, É. A.; Nagy, N. V.; Zsigó, É.; Kowol, C. R.; Arion, V. B.; Keppler, B. K.; Kiss, T.; *Eur. J. Inorg. Chem.* **2010** 1717–1728.

(36) Li, J.; Niu, C-S.; Li, X.; Doyle, T. W.; Chen, S-H. *Patent U.S.* **1998**, US5767134 A 19980616.

(37) a) Sava, G.; Jaouen, G.; Hillard, E. A.; Bergamo, A. *Dalton Trans.* **2012**, *41*, 8226–8234; b) Hait, W. N. *Cancer Res.* **2009**, *69*, 1263–1267; c) Gasser, G.; Ott, I.; Metzler-Nolte, N. *J. Med. Chem.* **2011**, *54*, 3–25.

(38) Kowol, C. R.; Eichinger, R.; Jakupec, M. A.; Galanski, M.; Arion, V. B.; Keppler, B. K. *J. Inorg. Biochem.* **2007**, *101*, 1946–1957.

(39) Arion, V. B.; Jakupec, M. A.; Galanski, M.; Unfried, P.; Keppler, B. K. *J. Inorg. Biochem.* **2002**, *91*, 298–305.

(40) Paolucci, G.; Zanella, A.; Bortoluzzi, M.; Sostero, S.; Longo, P.; Napoli, M. *J. Mol. Catal.* **2007**, *272*, 258–264.

(41) Ojida A.; Sakamoto T.; Inoue M.-A.; Fujishima S.-H.; Lippens G.; Hamachi I. *J. Am. Chem. Soc.* **2009**, *131*, 6543–6548.

(42) Bradley D.; William G.; Cullen A.; Fourie A.; Henning H.; Lawton M.; Mommsen W.; Nangu P.; Parker J.; Renison A. *Green Chem.* **2010** *12*, 1919–1921.

(43) a) Sunkel, K.; Hoffmuller, W.; Beck, W. *Z. Naturforsch.* **1998**, *53b*, 1365–1368; b) Poth, T.; Paulus, H.; Elias, H.; Dücker-Benfer, C.; van Eldik, R. *Eur. J. Inorg. Chem.* **2001**, 1361–1369; c) Yousef, R. I.; Bette, M.; Kaluderović, G. N.; Paschke, R.; Yiran, C.; Steinborn, D.; Schmidt, H. *Polyhedron* **2011**, *30*, 1990–1996; d) Carmona, D.; Lahoz, F. J.; Atencio, R.; Oro, L. A.; Lamata, M. P.; Viguri, F.; José, E. S.; Vega, C.; Reyes, J.; Joó, F.; Kathó, Á. *Chem. Eur. J.* **1999**, *5*, 1544–1564.

(44) Carmona, D.; Lamata, M. P.; Viguri, F.; Dobrinovich, I.; Lahoz, F. L.; Oro, L. A. *Adv. Synth. Catal.* **2002**, *344*, 499–502.

(45) Mabbs F.E., Collison D. *Electron Paramagnetic Resonance of d-Transition Metal Compounds*, Elsevier Science Publishers B.V., Amsterdam, 1992.

(46) Hu, K. N.; Song C. G.; Ju, H.-H.; Swager, T. M.; Griffin, R. G. *J. Am. Chem. Soc.* **2006** *128*, 11385–11390.

(47) Osheroff, N. *Biochim.Biophys. Acta* **1998**, *1400*, 1–2.

(48) Pelosi, G. *Open Crystallogr. J.* **2010**, *3*, 16–28.

(49) Williams, D. B. G.; Lawton, M. *J. Org. Chem.* **2010**, *75*, 8351–8354.

(50) Gran, G. *Acta Chem. Scand.* **1950**, *4*, 559–577.

(51) Irving, H. M.; Miles, M. G.; Pettit, L. D. *Anal. Chim. Acta* **1967**, *38*, 475–488.

(52) SCQuery, The IUPAC Stability Constants Database, Academic Software (Version 5.5)

(53) Sabatini, A.; Vacca, A.; Gans, P. *Talanta* **1974**, *21*, 53–77.

(54) Zékány, L.; Nagypál, I. in: *Computational Methods for the Determination of Stability Constants* (Ed.: D. L. Leggett), Plenum Press, New York, **1985**, p. 291–353.

(55) Rockenbauer, A.; Szabó-Plánka, T.; Arkosi, Zs.; Korecz, L. *J. Am. Chem. Soc.* **2001**, *123*, 7646–7654.

(56) Rockenbauer, A.; Korecz, L. *Appl. Magn. Reson.* **1996**, *10*, 29–43.

(57) Otwinowski, Z.; Minor, W, Methods in Enzymology, in C. W. Carter Jr., R. M. Sweet (Eds.), *Macromolecular Crystallography*, Part A, Vol. *276*, Academic Press, New York, **1997**, pp. 307−326.

(58) Sheldrick, G. M. *Acta Crystallogr.* A64 **2008**, 112–122.

(59) Burnett, M. N.; Johnson, G. K. ORTEPIII. Report ORNL-6895. OAK Ridge National Laboratory; Tennessee, **1996**.

For Table of Contents only